Cytoplasmic and nuclear Sw-5b synergistically induce plant immune responses to inhibit different viral infection steps

Hongyu Chen[1, 2, †], Xin Qian[1, 3, †], Xiaojiao Chen[1, 4, †], Tongqing Yang[1, 2], Mingfeng Feng[1, 2], Jing Chen[1, 2], Ruixiang Cheng[1, 2], Hao Hong[1, 2], Ying Zheng[1], Yuzhen Mei[5], Danyu Shen[1, 2], Yi Xu[1, 2], Min Zhu[1, 2], Xin Shun Ding[1] and Xiaorong Tao[1, 2, *]

[1] Department of Plant Pathology, College of Plant Protection, Nanjing Agricultural University, Nanjing 210095, P. R. China.

[2] Key Laboratory of Plant Immunity, Nanjing Agricultural University, Nanjing 210095, P. R. China.

[3] Huaiyin Institute of Agricultural Sciences of Xuhuai Region in Jiangsu ，Huaian 223001, Jiangsu, P. R. China.

[4] College of Plant Protection, Yunnan Agricultural University, Kunming 650201, Yunnan, P. R. China.

[5] State Key Laboratory of Rice Biology, Institute of Biotechnology, Zhejiang University, Hanghzou 310029, P. R. China.

[†] These authors contributed equally to this work.

*For Correspondence:

taoxiaorong@njau.edu.cn

Running Title

Sw-5b-mediated immunity against different viral infection steps

Abstract

Plant intracellular nucleotide binding-leucine-rich repeat (NLR) receptors play critical roles in mediating host immunity to pathogen attack. Successful virus infection in plant involves several essential steps including viral replication, intercellular and long-distance movement. How plant NLRs induce resistances against virus infection remains largely unknown. We demonstrated here that tomato NLR Sw-5b locates to cytoplasm and nucleus, respectively, to play different roles in inducing host resistances against tospovirus infection. The cytoplasmic Sw-5b functions to induce a strong cell death response to inhibit TSWV replication. This host response is, however, insufficient to block viral intercellular and long-distance movement. The nucleus-localized Sw-5b triggers a host defense that weakly inhibit viral replication but strongly impede virus intercellular and systemic movement. Furthermore, the cytoplasmic and nuclear Sw-5b act synergistically to confer a strong immunity to TSWV infection. Our finding adds a new knowledge to our current understanding on the plant NLRs-triggered immunity against virus infection.

Introduction

Plant innate immunity plays critical roles in host defense against pathogen invasions, and is triggered by cell-surface receptors or intracellular nucleotide-binding leucine-rich repeat (NLR) receptors (Soosaar et al., 2005; Dodds and Rathjen, 2010; Cui et al., 2015; Li et al., 2015; Jones et al., 2016; Kourelis and van der Hoorn, 2018; Kapos et al., 2019; van Wersch, 2020). Plant intracellular NLRs are the largest classes of resistance proteins that function to detect pathogen effectors, and to activate host immunity upon pathogen attack (Caplan et al., 2008a; Takken and Goverse, 2012; Li et al., 2015; Jones et al., 2016; Kourelis and van der Hoorn, 2018; Kapos et al., 2019). Plant NLRs typically contain an N-terminal domain, a central nucleotide-binding domain (NB), a nucleotide-binding adaptor (ARC domain shared by Apaf-1, certain resistance proteins, and CED-4), and a C-terminal leucine-rich repeat (LRR) domain (Ea and Jones, 1998; Jones et al., 2016; Ma et al., 2018; Wang et al., 2019a; Wang et al., 2019b; Ma et al., 2020). Based on the differences among the N-terminal domains, plant NLRs can be further divided into two main categories, known as the coiled-coil NLR (refers to as CNL) category and the Toll/interleukin-1 receptor NLR (TNL) category (Meyers et al., 2003; Collier and Moffett, 2009; Qi and Innes, 2013). The CC- or the TIR-domain-bearing NLRs have distinct genetic requirements and can regulate different functions in the downstream of defense signaling (Collier and Moffett, 2009; Qi and Innes, 2013; Horsefield et al., 2019; Jubic et al., 2019; van Wersch and Li, 2019; Wan et al., 2019).

Translocations of plant NLRs into proper subcellular compartments are critical for

the induction of innate immunity (Cui et al., 2015; van Wersch, 2020). Multiple plant NLRs and immune regulators, including tobacco N, Arabidopsis snc1, RRS1/RPS4, barley MLA10, and Arabidopsis EDS1, NPR1, have been shown to accumulate in both cytoplasm and nucleus, and for several nucleocytoplasmic NLRs accumulation in nucleus is required for triggering host resistance to pathogen infections (Deslandes et al., 2003; Burch-Smith et al., 2007; Shen et al., 2007; Wirthmueller et al., 2007; Tasset et al., 2010; Bai et al., 2012; Inoue et al., 2013; Padmanabhan et al., 2013). Wheat Sr33, a homolog of barley MLA10, however, was reported to accumulate in cytoplasm to induce host resistance against stem rust pathogen (Cesari et al., 2016). For potato Rx, a balanced cytoplasm and nucleus accumulation of Rx is needed to induce the host immunity (Slootweg et al., 2010; Tameling et al., 2010). Other studies have shown that Arabidopsis Rpm1 (Gao et al., 2011), RPS2 (Axtell and Staskawicz, 2003), RPS5 (Qi et al., 2012), rice Pit (Takemoto et al., 2012), and tomato Tm-2^2 (Chen et al., 2017; Wang et al., 2020) need to associate with plasma membrane in order to trigger cell death and host immunity. Latest studies have shown that the activated Arabidopsis ZAR1 can bind to cellular membrane, leading to a membrane leakage followed by cell death and host immunity (Wang et al., 2019a; Wang et al., 2019b). Flax L6 and M have been shown to accumulate in both Golgi apparatus and tonoplast, and these compartmentalized localizations are necessary for the induction of host resistance (Kawano et al., 2014). The re-distribution of potato R3a from cytosol to endosomal compartments is crucial for the induction of host resistance to *Phytophthora infestans* infection (Engelhardt et al., 2012). Different plant NLRs have

diverse subcellular localizations for their proper functions. However, how the compartmentalized localizations of plant NLRs specifically regulate defense signaling remain largely unknown.

Successful virus infection in plant requires viral replication in the initially infected cells followed by cell-to-cell and long-distance movement (Heinlein, 2015; Wang, 2015). After entering into plant cells, virus first encode multiple proteins needed for its replication. Once the initial replication is established, virus will encode specific protein(s), known as movement proteins (MPs), to traffic viral genome or virions into adjacent cells through plasmodesmata in cell walls, and then long-distantly into other parts of the plant to cause a systemic infection (Rao, 2002; Lucas, 2006; Taliansky et al., 2008). To date, multiple plant NLRs, conferring host resistance against plant viruses have been identified (Soosaar et al., 2005; Meier et al., 2019), but how these plant NLRs induce host resistance against virus infection remain largely unknown.

Tospovirus is one of the most devastating plant virus worldwide and poses serious threats to global food security (Kormelink et al., 2011; Scholthof et al., 2011; Oliver and Whitfield, 2016). Tomato NLR Sw-5b confers a strong resistance to tospovirus infection and has been widely used in tomato breeding projects to produce tospovirus resistant tomato cultivars (Brommonschenkel et al., 2000; Spassova M I, 2001; Turina et al., 2016; Zhu et al., 2019). Upon recognition of tospovirus movement protein, NSm, Sw-5b can trigger a hypersensitive response (HR) , which typically associated with localized cell death (Lopez et al., 2011; Hallwass et al., 2014; Peiro et al., 2014; De Oliveira et al., 2016; Zhao et al., 2016; Leastro et al., 2017). We have previously

shown that Sw-5b can confer a broad-spectrum resistance to American type tospoviruses, including type species of tospovirus-tomato spotted wilt virus (TSWV), through recognition of a conserved 21 amino acid PAMP-like region in the viral NSm protein (Zhu et al., 2017). Sw-5b carries an extended N-terminal *Solanaceae* domain (SD), a CC domain, a NB-ARC domain, and a LRR domain (Brommonschenkel et al., 2000; Spassova M I, 2001; Lukasik-Shreepaathy et al., 2012). Similar SDs have also been found in the Mi-1.2, R8, Rpi-blb2, and Hero (Milligan et al., 1998; Vos et al., 1998; Ernst et al., 2002; van der Vossen et al., 2005; Lukasik-Shreepaathy et al., 2012; Vossen et al., 2016). More recently, Seong and others reported that the extended CNL is evolved initially in the ancestor of *Asterids* and *Amaranthaceae*, predated the *Solanaceae* family (Seong et al., 2020). In the presence of the extended N-terminal SD, Sw-5b is in an autoinhibited state through multilayered interactions between SD, CC, NB-ARC, and LRR domains (Chen et al., 2016). For activation, Sw-5b adopts a two-step strategy to recognize NSm through SD and then LRR domain (Li et al., 2019). This two-step recognition strategy significantly enhances the sensitivity of the detection on TSWV NSm. Although Sw-5b is known to localize in both cytoplasm and nucleus (De Oliveira et al., 2016), the biological roles of the cytoplasm- and the nucleus-accumulated Sw-5b in host immunity signalling are unknown.

In this study, we investigated the subcellular distribution pattern of Sw-5b and the functions of the compartmentalized Sw-5b in the induction of host immunity to TSWV infection. We have determined here that cytoplasm- and nucleus-accumulated Sw-5b functions differently in inducing host defense response to inhibit different

tospovirus infection steps. The cytoplasmic Sw-5b can induce a strong cell death response to suppress TSWV replication, wheareas the nucleus-accumulated Sw-5b can induce a strong defense against viral intercellular movement and systemic infection. Combination of cytoplasmic and nuclear Sw-5b induces a synergistic and strong plant immunity against tospovirus infection. This finding has broad implications for future investigations on the roles of plant NLRs against different pathogen infection steps.

Results

Determination of Sw-5b subcellular localization pattern

Expression of YFP-Sw-5b in *N. benthamiana* leaves resulted in a strong HR cell death as well as Sw-5b (Chen et al., 2016; Zhu et al., 2017). To investigate the subcellular localization pattern of Sw-5b, we transiently expressed YFP and YFP-Sw-5b in *N. benthamiana* leaves, respectively, through agro-infiltration. Confocal Microscopy results showed that the YFP-Sw-5b fusion accumulated in both cytoplasm and nucleus in *N. benthamiana* leaf cells (Figure 1B, middle image). This subcellular localization pattern was similar to that of YFP (Figure 1B, left image). When a D857V mutation, which keeps Sw-5b in an autoactivated state (Chen et al., 2016), was introduced into Sw-5b to produce pYFP-Sw-5b^{D857V} and expressed in *N. benthamiana* leaves, the mutant YFP-Sw-5b^{D857V} fusion also accumulated in both cell cytoplasm and nucleus (Figure 1B, right image).

To investigate the subcellular localization pattern of Sw-5b in tomato leaf cells,

we transiently expressed YFP, YFP-Sw-5b, and YFP-Sw-5b^{D857V}, respectively, through particle bombardment. Confocal Microscopy results showed that these three proteins exhibited the same subcellular localization pattern as that in the *N. benthamiana* leaf cells (Figure 1C).

To further confirm the above results, we harvested *N. benthamiana* leaves expressing YFP-Sw-5b or YFP-Sw-5b^{D857V}. Leaf samples agro-infiltrated with the empty vector (p2300S) were also harvested and used as controls. Analyses of total protein, cytoplasm fractions, and nucleus fractions from these harvested leaves using Western blot assays showed that both YFP-Sw-5b and YFP-Sw-5b^{D857V} were accumulated in the cytoplasm and nucleus (Figure 1D).

Sw-5b recognizes TSWV NSm in cytoplasm

TSWV NSm is known to reside in cytoplasm and in plasmodesmata in cell walls, but not in nucleus (Kormelink et al., 1994; Feng et al., 2016). To determine where Sw-5b can recognize TSWV NSm, we fused a NES, a nes, a NLS or a nls signal peptide to the C-terminus of NSm-YFP to produce NSm-YFP-NES, NSm-YFP-nes, NSm-YFP-NLS, and NSm-YFP-nls, respectively. Transient expressions of these fusions in *N. benthamiana* leaves showed that NSm-YFP-NES accumulated exclusively in the cytoplasm, while NSm-YFP-NLS accumulated in the nucleus (Figure supplemental 1A). As expected, NSm-YFP-nes and NSm-YFP-nls showed the same accumulation pattern as that of NSm-YFP (Figure supplemental 1A). When Sw-5b was co-expressed with one of the above four fusions in *N. benthamiana* leaves

178 through agro-infiltration, the leaf tissues co-expressing Sw-5b and NSm-YFP-NES
179 (Sw-5b + NSm-YFP-NES), Sw-5b and NSm-YFP-nes (Sw-5b + NSm-YFP-nes), or
180 Sw-5b and NSm-YFP-nls (Sw-5b + NSm-YFP-nls) developed a strong HR cell death
181 (Figure supplemental 1B). In contrast, the leaf tissues co-expressing Sw-5b and
182 NSm-YFP-NLS (Sw-5b + NSm-YFP-NLS) did not. Western blot assays using an YFP
183 specific antibody confirmed that all the assayed proteins were expressed in the
184 infiltrated tissues (Figure supplemental 1C), indicating that Sw-5b recognizes NSm in
185 the cytoplasm.
186
187 **Sw-5b activity in cell death induction is enhanced in the cytoplasm but**
188 **suppressed in the nucleus**
189 To investigate the roles of the cytoplasmic and nuclear Sw-5b in the induction of cell
190 death and host immunity, we produced constructs to express YFP-Sw-5b,
191 NLS-YFP-Sw-5b, nls-YFP-Sw-5b, NES-YFP-Sw-5b, and nes-YFP-Sw-5b,
192 respectively, and then tested their abilities to elicit cell death and host immunity to
193 tospovirus infection. Transient expressions of these fusions in *N. benthamiana* leaves
194 showed that NES-YFP-Sw-5b accumulated exclusively in the cytoplasm, while
195 NLS-YFP-Sw-5b accumulated only in the nucleus (Figure 2A). In addition,
196 nes-YFP-Sw-5b and nls-YFP-Sw-5b showed the same accumulation pattern as that
197 shown by YFP-Sw-5b. We then tested cell death induction through co-expressions of
198 NSm and YFP-Sw-5b (NSm + YFP-Sw-5b), NSm and NES-YFP-Sw-5b (NSm +
199 NES-YFP-Sw-5b), NSm and nes-YFP-Sw-5b (NSm + nes-YFP-Sw-5b), NSm and

NLS-YFP-Sw-5b (NSm + NLS-YFP-Sw-5b), or NSm and nls-YFP-Sw-5b (NSm + nls-YFP-Sw-5b) in *N. benthamiana* leaves through agro-infiltration. Results of this study showed that the NSm + NES-YFP-Sw-5b-induced cell death was stronger than that induced by NSm + nes-YFP-Sw-5b or NSm + nls-YFP-Sw-5b co-expression (Figure 2B). In addition, the cell death induced by NSm + NLS-YFP-Sw-5b co-expression was suppressed (Figure 2B). Western blot results showed that the stronger cell death caused by NSm + NES-YFP-Sw-5b co-expression was not due to a greater accumulation of NES-YFP-Sw-5b in the leaves (Figure 2C). The ion leakage assay results (Figure 2D) agreed with the phenotype observation results, and indicated that co-expression of NSm + NES-YFP-Sw-5b in leaves lead to a greater ion leakage compared with that induced by the co-expression of NSm + nes-YFP-Sw-5b at 24 and 48 hours post agro-infiltration (hpai). The ion leakage caused by the co-expression of NSm + NLS-YFP-Sw-5b was significantly weaker than that caused by the co-expression of NSm + nls-YFP-Sw-5b (Figure 2D).

Cytoplasmic Sw-5b induces a strong host defense against tospovirus replication

Virus infection in plant starts with virus replication in the initially infected cells followed by spreading into adjacent cells for further infection. To monitor tospovirus replication in plant cells, we recently developed a TSWV mini-replicon-based reverse genetic system (Feng et al., 2020). In this study, co-expression of TSWV mini-replicon $SR_{(+)eGFP}$, $L_{(+)opt}$ (with a codon usage optimized RdRp), VSRs and NSm resulted in a cell-to-cell movement of $SR_{(+)eGFP}$. In contrast, co-expression of $SR_{(+)eGFP}$,

222 $L_{(+)opt}$, VSRs, and $NSm^{H93A\&H94A}$ mutant, a defective movement protein but can be
223 recognized by Sw-5b to cause a strong HR (Zhao et al., 2016), in cells resulted in the
224 expression of $SR_{(-)eGFP}$ in only single cells (Figure supplemental 2), thus dissecting the
225 viral replication from viral cell-to-cell movement. We then co-expressed $SR_{(+)eGFP}$,
226 $L_{(+)opt}$, VSRs, $NSm^{H93A\&H94A}$ mutant and one of the five proteins (i.e., Sw-5b,
227 NES-Sw-5b, nes-Sw-5b, NLS-Sw-5b, nls-Sw-5b) in *N. benthamiana* leaves. Leaves
228 co-expressing $SR_{(+)eGFP}$, $L_{(+)opt}$, VSRs, $NSm^{H93A\&H94A}$ mutant and p2300 (empty vector,
229 EV) were used as controls. The results showed that in the presence of Sw-5b or one of
230 its derivatives, the expression of $SR_{(+)eGFP}$ was strongly suppressed compared with
231 that expressed in the presence of EV (Figure 3A). It is noteworthy that the expression
232 of $SR_{(+)eGFP}$ was less inhibited in the presence of NLS-Sw-5b (Figure 3A). Western
233 blot result indicated that the GFP accumulation of $SR_{(+)eGFP}$ was strongly inhibited in
234 the presence of Sw-5b, NES-Sw-5b, nes-Sw-5b or nls-Sw-5b compared with that
235 expressed in the presence of NLS-Sw-5b or EV (Figure 3B). This finding indicates
236 that the cytoplasmic Sw-5b can inhibit $SR_{(+)eGFP}$ expression, possibly through
237 induction of a host defense against TSWV replication.
238
239 **Sw-5b induces a host defense against viral NSm intercellular movement**
240 In our previous study, we used pmCherry-HDEL//NSm-GFP vector (Figure 4A) to
241 investigate TSWV NSm cell-to-cell movement (Feng et al., 2016). The expressed
242 mCherry-HDEL binds ER membrane in the initial cells but NSm-eGFP traffics
243 between cells. To investigate whether the Sw-5b-induced host defense can affect

TSWV NSm cell-to-cell movement, we co-expressed mCherry-HDEL, NSm-GFP, and Sw-5b or mCherry-HDEL, NSm-GFP, and EV in *N. benthamiana* leaves through agro-infiltration. Under the fluorescence microscope, both NSm-GFP and mCherry-HDEL were found in single cells in the presence of Sw-5b. In the presence of EV, however, NSm-GFP moved into multiple cells, while mCherry-HDEL accumulated in the initial cells (Figure 4B, upper two panels). The result suggested that Sw-5b elicited a defense that strongly inhibited cell-to-cell movement of viral NSm.

Sw-5b in the nucleus but not in the cytoplasm triggers a defense against NSm cell-to-cell movement

To determine the effects of the cytoplasmic and nuclear Sw-5b on host defense against TSWV NSm intercellular movement, we co-expressed mCherry-HDEL and NSm-GFP with NES-Sw-5b, nes-Sw-5b, NLS-Sw-5b, or nls-Sw-5b in *N. benthamiana* leaves via agro-infiltration. The results showed that in the presence of NLS-Sw-5b, the cell-to-cell movement of NSm-GFP was inhibited (Figure 4B). Similar results were also obtained in the leaves co-expressing mCherry-HDEL and NSm-GFP with nls-YFP-Sw-5b or nes-YFP-Sw-5b (Figure supplemental 3). In the presence of NES-YFP-Sw-5b, however, NSm-GFP did move into surrounding cells. (Figure 4B). This finding indicates that the Sw-5b in the nucleus but not in the cytoplasm induced a host defense that inhibited TSWV NSm cell-to-cell movement.

Nuclear Sw-5b confers host immunity to TSWV systemic infection

To dissect the host immunity induced by the cytoplasmic and the nuclear Sw-5b, we generated transgenic *N. benthamiana* lines expressing YFP-Sw-5b, NES-YFP-Sw-5b, nes-YFP-Sw-5b, NLS-YFP-Sw-5b, and nls-YFP-Sw-5b, respectively (Table supplemental 1 and Table supplemental 2). After inoculation of these transgenic lines with TSWV-YN isolate, the EV (control) transgenic plants developed typical viral symptoms including stunt, leaf curl and mosaic at 7 to 15 days post inoculation (dpi). The NES-YFP-Sw-5b transgenic plants developed a strong HR trailing in the systemic leaves by 7 to 15 days post inoculation (dpi) (Figure 5A and Figure supplemental 4A), suggesting that NES-YFP-Sw-5b transgenic plant did not block TSWV systemic infection and caused virus infection-related systemic HR. In contrast, no systemic virus infection symptoms were observed in the YFP-Sw-5b and the nes-YFP-Sw-5b transgenic plants. The RT-PCR agreed with the symptom observation results and showed that TSWV-YN genomic RNA was accumulated in the systemic leaves of the TSWV-YN-inoculated NES-YFP-Sw-5b or the EV transgenic plants, but not in the systemic leaves of the TSWV-YN-inoculated YFP-Sw-5b or nes-YFP-Sw-5b transgenic plants (Figure 5C and Figure supplemental 4B). Also in this study, the TSWV-YN-inoculated NLS-YFP-Sw-5b or nls-YFP-Sw-5b transgenic plants did not show virus like symptoms in their systemic leaves by 7-15 dpi (Figure 5A, and Figure supplemental 4A). The RT-PCR result confirmed that TSWV-N genomic RNA had not accumulated in the systemic leaves of the NLS-YFP-Sw-5b or the nls-YFP-Sw-5b transgenic plants (Figure 5C, and Figure supplemental 4B),

288 indicating that the nuclear Sw-5b is responsible for the host immunity against TSWV
289 systemic infection.
290
291 **Silencing *importin α1, α2* and *β* expression abolished Sw-5b nucleus**
292 **accumulation and host resistance to TSWV systemic infection**
293 *Importins* play important roles in translocating proteins from cytoplasm into nucleus
294 (Chook and Blobel, 2001; Kanneganti et al., 2007). To determine the functions of
295 importin α1, α2 and β in Sw-5b nucleus localization, we silenced *importin α1, α2, β,*
296 *α1* and *α2,* and *α1* and *α2* and *β* expressions, respectively, in *N. benthamiana* leaves
297 using a tobacco rattle virus (TRV)-based virus-induced gene silencing (VIGS) vector,
298 and then transiently expressed YFP-Sw-5b in these plants. Analyses of these plants
299 through RT-PCR using gene specific primers showed that silencing of these
300 *importin* genes in *N. benthamiana* leaves was successful (Figure supplemental 5A).
301 However, silencing individual *importin* gene or both *importin α1* and *α2* was not
302 enough to block the nucleus accumulation of YFP-Sw-5b (Figure 6A). In contrast,
303 after *importin α1, α2* and *β* were all silenced through VIGS, the nucleus accumulation
304 of YFP-Sw-5b was inhibited (Figure 6A, the middle image in the bottom panel).
305 To investigate the effects of nuclear import defected Sw-5b on host immunity to
306 TSWV systemic infection, we silenced these *importin* genes in the Sw-5b transgenic
307 *N. benthamiana* plants as described above, and then inoculated them with TSWV. The
308 results showed that the plants silenced for *importin α1, α2,* and *β* gene, individually,
309 did not show TSWV systemic infection (Figure 6B and Figure supplemental 5B). In

310 addition, the transgenic plants silenced for both *importin α1* and *α2* genes also did not
311 show TSWV systemic infection (Figure 6B and Figure supplemental 5B). In contrast,
312 after silencing *importin α1*, *α2* and *β* together, the plants developed clear TSWV
313 symptoms in systemic leaves followed by HR (Figure 6B, white arrow and Figure
314 supplemental 5B), indicating that the nucleus accumulation of Sw-5b is indispensable
315 for the induction of host immunity against TSWV systemic infection.
316
317 **The cytoplasmic and the nuclear Sw-5b act synergistically to confer a strong**
318 **immunity to TSWV infection in *N. benthamiana***
319 To investigate whether cytoplasm-targeted and nucleus-targeted Sw-5b have joint
320 effects on the defense against TSWV infection, we constructed a $M_{(-)opt}$-$pSR_{(+)eGFP}$
321 vector by inserting a cassette expressing optimized TSWV M genomic sequence
322 (Feng et al., 2020) into the $pSR_{(+)eGFP}$ mini-replicon to express NSm, N, and eGFP
323 simultaneously in the same cells (Figure 7A). The construct $M_{(-)opt}$-$pSR_{(+)eGFP}$ couples
324 the functions for both viral replication and viral cell-to-cell movement, mimicking the
325 virus infection in plant leaves. After co-expressing this vector, the $L_{(+)opt}$ and the EV in
326 *N. benthamiana* leaves through agro-infiltration, the eGFP fluorescence was observed
327 in many cells, due to the presence of the NSm movement protein and the $RdRp_{opt}$
328 (Figure 7B, upper left image). When $M_{(-)opt}$-$SR_{(+)eGFP}$, $L_{(-)opt}$ and Sw-5b were
329 co-expressed in *N. benthamiana* leaves, the eGFP fluorescence was hardly detected
330 and some were observed only in single leaf cells (Figure 7B upper right image, Figure
331 supplemental 6A and B). When $M_{(-)opt}$-$SR_{(+)eGFP}$, $L_{(+)opt}$ and NES-Sw-5b were

co-expressed in *N. benthamiana* leaves, the eGFP fluorescence was observed in clusters of a few cells (Figure 7B, Figure supplemental 6A), indicating that limited cell-to-cell movement had occurred in these leaves (Figure supplemental 6B). When $M_{(-)opt}$-$SR_{(+)eGFP}$, $L_{(+)opt}$ and NLS-Sw-5b were co-expressed in leaves, a few of eGFP fluorescence were detected but they were in single cells only. When leaves co-expressing $M_{(-)opt}$-$SR_{(+)eGFP}$, $L_{(+)opt}$ and NES-Sw-5b + NLS-Sw-5b, the eGFP fluorescence was also hardly detected and some were observed only in single leaf cells. Western blot results showed that more eGFP had accumulated in the leaves co-expressing $M_{(-)opt}$-$SR_{(+)eGFP}$, $L_{(+)opt}$, and EV, followed by the leaves co-expressing $M_{(-)opt}$-$SR_{(+)eGFP}$, $L_{(+)opt}$, and NLS-Sw-5b, and then the leaves co-expressing $M_{(-)opt}$-$SR_{(+)eGFP}$, $L_{(+)opt}$, and NES-Sw-5b. Much less eGFP had accumulated in the leaves co-expressing $M_{(-)opt}$-$SR_{(+)eGFP}$, $L_{(+)opt}$, and NLS-Sw-5b + NES-Sw-5b, and in the leaves co-expressing $M_{(-)opt}$-$SR_{(+)eGFP}$, $L_{(+)opt}$, and Sw-5b (Figure 7C and D). The accumulation of eGFP was lower in the leaves co-expressing NES-Sw-5b + NLS-Sw-5b than that in the leaves co-expressing NES-Sw-5b or NLS-Sw-5b (Figure 7C and D), indicating that NES-Sw-5b and NLS-Sw-5b have additive role in mediating host immunity against different TSWV infection steps.

The ARC and LRR domain control Sw-5b cytoplasm localization whereas the SD domain controls its nucleus localization

Sw-5b has an extended N-terminal SD domain, a CC domain, a NB-ARC domain, and a C-terminal LRR domain (Chen et al., 2016). To determine the roles of these

354 domains in Sw-5b subcellular localization, we produced vectors carrying individual
355 domains fused with the YFP, and then expressed them individually in *N. benthamiana*
356 leaves via agro-infiltration (Figure 8A). Under the confocal microscope, the YFP-SD,
357 YFP-CC, and YFP-NB fusion were found in both cytoplasm and nucleus (Figure 8A
358 and B). In contrast, the YFP-ARC and YFP-LRR fusion were found exclusively in the
359 cytoplasm. In addition, the YFP-NB-ARC, YFP-CC-NB, and YFP-CC-NB-ARC
360 fusion were found mostly in the cytoplasm. The YFP-NB-ARC-LRR (112 kDa)
361 fusion accumulated exclusively in the cytoplasm, and the YFP-CC-NB-ARC-LRR
362 fusion accumulated mainly in the cytoplasm (Figure 8A and B; Supplemental figure
363 7). These results indicate that the CC and the NB domain are likely insufficient to
364 traffic the fusions into the nucleus. Because the YFP-SD-CC fusion accumulated in
365 both cytoplasm and nucleus, and the YFP-SD-CC-NB-ARC-LRR fusion accumulated
366 in both cytoplasm and nucleus (Figure 8B). Based on these observations we consider
367 that the ARC and the LRR domain are important for Sw-5b cytoplasm accumulation
368 and the SD domain is important for Sw-5b nucleus accumulation.
369

370 **Discussion**

371 In this report, we provide evidence to show that the cytoplasm-accumulated and the
372 nucleus-accumulated Sw-5b, a tomato immune receptor, play different roles in
373 inducing host defense against tospovirus infection in plant. The cytoplasmic Sw-5b
374 functions to induce a strong cell death response to inhibit TSWV replication. This
375 host response is, however, insufficient to block virus intercellular and long-distance

376 movement. The nuclear-localized Sw-5b triggers a host defense that weakly inhibit
377 viral replication but strongly inhibit tospovirus intercellular and systemic movement.
378 The finding suggest that tomato Sw-5b NLR induces different type of resistances in
379 cell compartment-specific manner to inhibit different tospovirus infection steps.
380 Furthermore, the cytoplasmic and the nuclear Sw-5b act synergistically to confer a
381 strong host immunity to TSWV infection in plant.

382 Through CLSM and fractionation analyses, we have now determined that Sw-5b
383 accumulates in both cytoplasm and nucleus in *N. benthamiana* and tomato leaf cells.
384 We have also determined that the forced cytoplasm accumulation of Sw-5b can
385 induce a stronger cell death than that caused by the accumulation of Sw-5b in both
386 cytoplasm and nucleus. While, the cell death induced by the forced nucleus
387 accumulation of Sw-5b was significantly weakened. It was shown previously that the
388 Sw-5b NB-ARC-LRR region can induce HR cell death in plant (Chen et al., 2016). In
389 this study we showed that Sw-5b YFP-NB-ARC-LRR (112 kDa) accumulates in
390 cytoplasm exclusively (Figure 9B). Barley MLA10 has been shown to accumulate in
391 both cytoplasm and nucleus, and the forced cytoplasm accumulation of MLA10
392 enhance cell death signaling, while the forced nucleus accumulation of MLA10
393 inhibits its activity to induce cell death (Bai et al., 2012). Because both MLA10 and
394 Sw-5b activity on cell death signaling are enhanced in the cytoplasm but suppressed
395 in the nucleus, we speculate that, for both MLA10 and Sw-5b, the cytoplasm
396 accumulation is crucial for the initiation and/or amplification of the cell death
397 signaling. The CC and the TIR domain of several plant NLRs have been shown to

trigger cell death (Swiderski et al., 2009; Krasileva et al., 2010; Bernoux et al., 2011; Collier et al., 2011; Maekawa et al., 2011; Bai et al., 2012; Chen et al., 2017; Wang et al., 2020). Analyses of the three dimensional structures of Arabidopsis ZAR1 resistosome have also shown that its CC domain can form pentamer structures that was able to target into host cell membranes, leading to ion leakage and cell death (Wang et al., 2019a; Wang et al., 2019b). Our finding together with recent findings from ZAR1 resistosome lead to a new direction in the future to investigate whether Sw-5b and other plant NLRs such as MLA10 target to host cytoplasmic membranes and which specific membranes to cause the cell death.

Successful virus infection in host plants involves virus replication followed by intercellular and long-distance movement (Lucas, 2006; Heinlein, 2015; Wang, 2015). In this study, we analyzed Sw-5b-mediated immunity against TSWV replication using a TSWV mini-replicon system and a movement defective NSm mutant. Our results showed that the forced cytoplasm accumulation of Sw-5b can induce a strong host defense against virus replication in cells. This finding implies that cytoplasm is one of the main source of defense signaling against TSWV replication. The defense signaling generated in nucleus can only induce a weak defense against TSWV replication. Therefore, the nuclear localized Sw-5b is only partially responsible for the induction of host defense against TSWV replication. It is also possible that this nuclear localized Sw-5b-induced weak host response is caused by a trace of NLS-YFP-Sw-5b maintained in the cytoplasm that maybe below the detection limit of Confocal

Microscope. Because cell death is associated with ROS burst, further investigations are needed to determine if the inhibition of virus replication is caused by the toxicity of ROS on viral replicase or other proteins associated with virus replication in cells.

Plant virus encodes specific movement protein(s) to traffic viral genome between cells and then leaves to cause systemic infection (Rao, 2002; Lucas, 2006; Taliansky et al., 2008). We reported previously that TSWV NSm alone can move between plant cells (Feng et al., 2016). In this study, we investigated the effect of the Sw-5b-mediated host defence on TSWV intercellular movement. Through this study, we have determined that after the recognition of NSm, Sw-5b receptor induced a strong reaction to block NSm intercellular trafficking. Previous reports have some indications on the role of plant NLRs in viral movement. Nevertheless it has no direct evidence showing that plant NLRs induce resistance against viral movement. Deom and colleagues had shown that the 9.4-kDa fluorescein isothiocyanate-labeled dextran was unable to move between cells in the transgenic tobacco *N* leaves expressing tobacco mosaic virus (TMV) movement protein at 24°C, an HR-permissive temperature (Deom et al., 1991). However, that study did not involve a TMV Avr protein. In a different report, TMV-GFP showed a limited cell-to-cell movement in leaves of tobacco cv. Sumsan NN at 33°C, an HR-nonpermissive temperature (Canto and Palukaitis, 2002). Li and colleagues found that after the treatment of SMV-inoculated Jidou 7 resistant plants with a callose synthase inhibitor, the plants showed enlarged HR lesions (Li et al., 2012). The soybean *Rsv3* induced extreme

resistance. However, after this extreme resistant soybean line was treated with a callose synthase inhibitor, the plants developed HR lesions upon SMV-G5H inoculation (Seo et al., 2014). These reports indicate that plant NLRs likely involves the defense against viral movement. Here we provide the direct evidence that Sw-5b NLR can induce a strong defense response to impede NSm intercellular trafficking. More importantly, we have determined that the induction of host immunity to TSWV intercellular movement requires the accumulation of Sw-5b in nucleus. Although the cytoplasmic Sw-5b can induce a strong cell death response, it cannot prevent TSWV NSm cell-to-cell movement. Consequently, we propose that nucleus is a key compartment to generate defense signaling to block TSWV cell-to-cell movement.

In this study, although the NES-YFP-Sw-5b transgenic *N. benthamiana* plants showed a HR trailing response upon TSWV infection, they were unable to stop TSWV systemic infection. Based on this finding, we conclude that HR cell death alone is not sufficient to block TSWV long-distance movement. In our study, the NLS-YFP-Sw-5b transgenic plants were resistant to TSWV systemic infection. After silencing the expressions of *importin* $\alpha 1$, $\alpha 2$ and β simultaneously to inhibit the nucleus accumulation of Sw-5b, however, the resistance to TSWV systemic infection was abolished. These findings indicate that the Sw-5b-mediated resistance signaling against viral systemic infection is generated in nucleus. Some plant NLRs are known to interact with specific transcription factors in nucleus upon recognition of pathogen effectors (Cui et al., 2015; Kapos et al., 2019). The immune regulator EDS1 has also been shown to accumulate in nucleus to reprogram RNA transcription (Garcia et al.,

464 2010; Heidrich et al., 2011; Cui et al., 2015; Lapin et al., 2020). How Sw-5b regulates
465 host immunity in nucleus requires further investigations.

466 Several plant immune receptors and immune regulators, including, e.g. potato Rx
467 (Slootweg et al., 2010; Tameling et al., 2010), tobacco N (Burch-Smith et al., 2007;
468 Caplan et al., 2008b), barley MLA10 (Shen et al., 2007), Arabidopsis RRS1-R/RPS4,
469 and snc1 (Deslandes et al., 2003; Wirthmueller et al., 2007; Cheng et al., 2009), as
470 well as Arabidopsis NPR1 (Katagiri and Tsuda, 2010), and EDS1 (Lapin et al., 2020)
471 have been found to be nucleocytoplasmic. For some of them, nuclear accumulation of
472 NLRs are required for the induction of plant immunity to pathogen attacks. Moreover,
473 the MLA10-YFP-NES fusion was found to induce a strong cell death response, but
474 not a strong host resistance to powdery mildew fungus infection. In contrast, the
475 MLA10-YFP-NLS fusion inhibited its activity to induce a cell death response, but
476 caused a host immunity to this pathogen (Bai et al., 2012). In many plant-pathogen
477 interactions, cell death responses can be uncoupled from disease resistance
478 (Bendahmane et al., 1999; Gassmann, 2005; Coll et al., 2010; Heidrich et al., 2011).
479 This separation raises questions about how host resistance prevents pathogen invasion
480 and what are the roles of cell death during pathogen infection. It is unclear whether
481 the MLA10-YFP-NES-induced cell death has some inhibitory effects on powdery
482 mildew fungus infection. In this study, we determined that cytoplasm- and
483 nuclear-accumulation of Sw-5b have different functions. The cytoplasm-accumulated
484 Sw-5b induces a strong defense against virus replication, whereas the
485 nuclear-accumulated Sw-5b induced an inhibition of virus cell-to-cell and long

distance movement. Both cytoplasmic and nuclear Sw-5b are needed to confer a synergistic defense against tospovirus infection. We have also determined that Sw-5b NRC, LRR, and SD domains are important to regulate the proper subcellular localization of Sw-5b and the proper nucleoplasmic distribution of Sw-5b is needed to elicit full immune responses to inhibit different TSWV infection steps.

Based on the above results, we have created a working model for the Sw-5b NLR-induced host resistance against TSWV replication, and intercellular and long-distance movement in plant (Figure 9). Upon recognition of NSm in cytoplasm, Sw-5b switched from an autoinhibited state to an activated state. The activated Sw-5b accumulated in both the cytoplasm and the nucleus. The cytoplasm-accumulated and the nucleus-accumulated Sw-5b play different roles in inducing host immunity against TSWV infection. The cytoplasmic Sw-5b functions to induce a cell death response to inhibit TSWV replication, while the nuclear Sw-5b functions to induce a weak host defense against TSWV replication, but a strong defense against TSWV cell-to-cell and long-distance movement. The concerted defense signaling generated in the cytoplasm and nucleus resulted in a strong host resistance to tospovirus infection.

Materials and Methods

Plasmid construction

p2300S-YFP-Sw-5b was from a previously described source (Chen et al., 2016). Different domains of Sw-5b were PCR-amplified from p2300S-Sw-5b (Chen et al.,

2016) and cloned individually behind the *YFP* gene in the p2300S vector using a two-step overlap PCR procedure as described (Li et al., 2019). All the primers used in this study are listed in Table supplemental 3.

To visualize the subcellular localization patterns of various fusion proteins, a SV40 T-Ag-derived nuclear localization signal (NLS, QPKKKRKVGG) (Lanford and Butel, 1984) or a PK1 nuclear export signal (NES, NELALKLAGLDINK) (Wen et al., 1995) was fused to the N-terminus of YFP-Sw-5b or the C-terminus of NSm-YFP, as described (Kong et al., 2017), to produce pNES-YFP-Sw-5b, pNLS-YFP-Sw-5b, pNSm-YFP-NES, and pNSm-YFP-NLS, respectively. In addition, YFP-Sw-5b and NSm-YFP were fused individually with a mutant NLS (nls, QPKKTRKVGG) or a mutant NES (nes, NELALKAAGADANK) to produce pnes-YFP-Sw-5b, pnls-YFP-Sw-5b, pNSm-YFP-nes, and pNSm-YFP-nls. The constructs were then transformed individually into *Agrobacterium tumefaciens* strain GV3101 cells.

Transient gene expression, stable plant transformation, and virus inoculation

Nicotiana benthamiana were grown in soil in pots inside a greenhouse maintained at 25°C and a 16 h light/8 h dark photoperiod. Six-to-eight week-old *N. benthamiana* plants were used for various assays. Transient gene expression assays were performed in *N. benthamiana* leaves through agro-infiltration using Agrobacterium cultures carrying specific expressing constructs as described previously (Feng et al., 2016; Ma et al., 2017). Transgenic *N. benthamiana* lines expressing YFP-Sw-5b or its derivatives were made using constructs with a 35S promoter or a Sw-5b native

promoter via a standard leaf-disc transformation method (Chen et al., 2016). The resulting transgenic *N. benthamiana* lines were named as NES-YFP-Sw-5b, NLS-YFP-Sw-5b, nes-YFP-Sw-5b, nls-YFP-Sw-5b, YFP-Sw-5b, and EV (transformed with an empty vector), respectively. Inoculation of transgenic *N. benthamiana* plants with TSWV was done by rubbing plant leaves with TSWV-YN isolate-infected crude saps as described (Zhu et al., 2017). TRV-mediated VIGS in *N. benthamiana* plants was done as described (Ma et al., 2015). The agro-infiltrated or the virus-inoculated plants were grown inside a growth chamber maintained at 25/23 °C (day/night) with a 16/8 h light and dark photoperiod.

Particle bombardment

The particle bombardment is described (Feng et al., 2016). Briefly, 60 mg Tungsten M-10 microcarrier (Bio-RAD) was placed into a 1.5 ml Eppendorf tube with 1 mL 70% ethanol. The tube was vortexes for 3 minutes, and then stood at room temperature for 15 minutes. After centrifuge at low speed for 5 seconds, the supernatant was removed and the pellet was rinsed with 70% ethanol for 3 times. One mL 50% sterile glycerol solution was added and divided Tungsten M-10 microcarrier into 50 µl. Five µg pRTL2-YFP, pRTL2-YFP-Sw-5b or pRTL2-YFP-Sw-5bD857V plasmid DNA, 50 µl of 2.5 M CaCl2, and 20 µl of 0.1 M spermidine, respectively were added and mixed with microcarrier. After centrifuge at low speed for 5 seconds and the supernatant removed. The pellet was resuspended in 200 µl 70% ethanol and centrifugation as described above. Use 48 µl of 100% ethanol to resuspend the

552 tungsten particle::plasmid DNA complexes, and load 15 48 µl mixture onto the center
553 of carrier (Bio-RAD), air dry, and use He/1000 particle transport system (BIO-RAD)
554 to bombard tomato leaves harvested from 3- or 4-week-old of Money Marker. The
555 bombarded leaves were incubated in Petri dishes for 24 hours at 25℃ followed with
556 Confocal Microscope analysis.

557

558 **Trypan blue staining**

559 *N. benthamiana* leaves were harvested at 3 days post agro-infiltration (dpai) and
560 boiled for 5 min in a 1.15:1 (v/v) mixed ethanol and trypan blue staining solution (10
561 g phenol, 10 mL glycerol, 10 mL lactic acid, and 20 mg trypan blue in 10 mL distilled
562 water). The stained leaves were then de-stained in a chloral hydrate solution (2.5 g per
563 mL distilled water) as described (Bai et al., 2012).

564

565 **Electrolyte leakage assay**

566 Electrolyte leakage assay was performed as previously described (Mittler et al., 1999;
567 Zhu et al., 2017) with slight modifications. Briefly, five leaf discs (9 mm in diameter
568 each) were taken from the agro-infiltrated leaves per treatment and at various dpai.
569 The harvested leaf discs from a specific treatment were floated on a 10 mL distilled
570 water for 3 h at room temperature (RT), and the conductivity of each bathing water
571 was measured (referred to as value A) using a Multiparameter Meter as instructed
572 (Mettler Toledo, Zurich, Switzerland). After the first measurement, the leaf discs were
573 returned to the bathing water and incubated at 95°C for 25 min. After cooling down to

RT, the conductivity of each bathing sample was measured again (referred to as value B). The ion leakage was expressed as the ratio determined by value A/value B × 100. The mean value and standard error of each treatment were calculated using the data from three biological replicates per treatment at each sampling time point.

Confocal laser scanning microscopy

Tissue samples were collected from the leaves transiently expressing YFP-Sw-5b or one of the fusion proteins at 24–36 hours post agro-infiltration (hpai). The collected tissue samples were mounted in water between a glass slide and a coverslip. Images of individual samples were captured under a Carl Zeiss LSM 710 confocal laser scanning microscope. YFP fusions were excited at 488 nm and the emission was captured at 497–520 nm. The resulting images were further processed using the Zeiss 710 CLSM software followed by the Adobe Photoshop software (San Jose, CA, USA).

Nucleus and cytoplasm fractionations

N. benthamiana leaf tissues (1 g per sample), representing a specific treatment, were collected at 24 hpai, frozen in liquid nitrogen, ground to fine powders, and then homogenized in 2 mL (per sample) extraction buffer 1 (20 mM Tris-HCl, pH 7.5, 20 mM KCl, 2.5 mM $MgCl_2$, 2 mM EDTA, 25% glycerol, 250 mM sucrose, 1×Protease Inhibitor Cocktail, and 5 mM DTT). The resulting lysate was filtered through 30 μm filters to remove debris, and the filtrate was centrifuged at 2,000 × *g* for 5 minutes to

pellet nuclei. The supernatant from a sample was transferred into a new tube and centrifuged at 10,000×*g* for 10 min. The resulting supernatant was used as the cytoplasm fraction. The nuclei containing pellet was resuspended in 5 mL extraction buffer 2 (20 mM Tris-HCl, pH 7.4, 25% glycerol, 2.5 mM MgCl2, and 0.2% Triton X-100), centrifuged for 10 min at 2,000 × *g* followed by 4-6 cycles of resuspension and centrifugation as described above. The resulting pellet was resuspended again in 500 μl extraction buffer 3 (20 mM Tris-HCl, pH 7.5, 0.25 M sucrose, 10 mM MgCl2, 0.5% Triton X-100, and 5 mM β-mercaptoethanol). The nuclei fraction was carefully layered on the top of 500 mL extraction buffer 4 (20 mM Tris-HCl, pH 7.5, 1.7 M sucrose, 10 mM MgCl2, 0.5% Triton X-100, 1×Protease Inhibitor Cocktail, and 5 mM β-mercaptoethanol), and then centrifuged at 16,000 × *g* for 1 h. The resulting pellet was resuspended in 500 μL extraction buffer 1 and stored at −80°C until use or used immediately for SDS-PAGE assays. All the processes were performed on ice or at 4°C. In this study, actin and histone H3 were used as the cytoplasmic and the nuclear markers, respectively.

Western blot and co-immunoprecipitation assays

Western blot and co-immunoprecipitation assays were performed as described (Zhu et al., 2017). Briefly, agro-infiltrated leaf samples (1 g per sample) were harvested and homogenized individually in pre-chilled mortars with pestles in 2 mL extraction buffer [10% (v/v) glycerol, 25 mM Tris, pH 7.5, 1 mM EDTA, 150 mM NaCl, 10 mM DTT, 2% (w/v) polyvinylpolypyrrolidone, and 1 × protease inhibitor cocktail (Sigma,

Shanghai, China)]. Each crude slurry was transferred into a 2 mL Eppendorf tube, and spun for 2 min at full speed in a refrigerated microcentrifuge. The supernatant was transferred into a clean 1.5 mL Eppendorf tube and spun for 10 min at 4°C. For Western blot assays, 50 μL supernatant from a sample was mixed with 150 μL Laemmli buffer, boiled for 5 min, and analyzed in SDS-PAGE gels through electrophoresis. For immunoprecipitation assays, 1 mL supernatant was mixed with 25 μL GFP-trap agarose beads (ChromoTek, Planegg-Martinsried, Germany), incubated for 2 h at 4°C on an orbital shaker, and then pelleted through low speed centrifugation. The blots were probed with a 1:2,500 (v/v) diluted anti-YFP antibody or other specific antibodies followed a 1:10,000 (v/v) diluted horseradish peroxidase (HRP)-conjugated goat anti-rabbit or a goat anti-mouse antibody (Sigma-Aldrich, St. Louis, MO, USA). The detection signal was developed using the ECL substrate kit as instructed (Thermo Scientific, Hudson, NH, USA).

RT-PCR detection of TSWV infection

Total RNA was extracted from TSWV-inoculated *N. benthamiana* plant leaves using an RNA Purification Kit (Tiangen Biotech, Beijing, China), and then treated with RNase-free DNase I (TaKaRa, Dalian, China). First-strand cDNA was synthesized using a TSWV-specific primer (Supplementary Table 4). PCR reactions were as follows: initial denaturation at 94°C for 2 min followed by 35 cycles of 94°C for 30 s, 52°C for 30 s, and 72°C for 1 min. The final extension was 72°C for 10 min. The resulting PCR products were visualized in 1.0% (w/v) agarose gels through

electrophoresis.

Acknowledgments

This work was supported by the National Natural Science Foundation of China (31630062, 31925032 and 31870143), the Fundamental Research Funds for the Central Universities (JCQY201904 and KYXK202012), Youth Science and Technology Innovation Program to XT.

Author contributions

Hongyu Chen, Xin Qian and Xiaojiao Chen, Data curation, Formal analysis, Validation, Methodology, Writing - original draft, Writing - review and editing; Tongqing Yang, Mingfeng Feng, Jing Chen, Ruixiang Cheng, Hao Hong, Ying Zheng, Yuzhen Mei, Danyu Shen, Yi Xu, Min Zhu Data curation, Methodology; Xin Shun Ding, Methodology, Writing - review and editing; Xiaorong Tao, Investigation, Writing - original draft, Writing - review and editing.

Competing interests:

The authors declare that nocompeting interests exist.

Data availability

All data produced in this study are presented in this manuscript or as the supporting files

References

Axtell, M.J., and Staskawicz, B.J. (2003). Initiation of RPS2-specified disease resistance in Arabidopsis is coupled to the AvrRpt2-directed elimination of RIN4. Cell **112,** 369-377.

Bai, S., Liu, J., Chang, C., Zhang, L., Maekawa, T., Wang, Q., Xiao, W., Liu, Y., Chai, J., Takken, F.L., Schulze-Lefert, P., and Shen, Q.H. (2012). Structure-function analysis of barley NLR immune receptor MLA10 reveals its cell compartment specific activity in cell death and disease resistance. PLoS Pathog **8,** e1002752.

Bendahmane, A., Kanyuka, K., and Baulcombe, D.C. (1999). The Rx gene from potato controls separate virus resistance and cell death responses. Plant Cell **11,** 781-792.

Bernoux, M., Ve, T., Williams, S., Warren, C., Hatters, D., Valkov, E., Zhang, X., Ellis, J.G., Kobe, B., and Dodds, P.N. (2011). Structural and functional analysis of a plant resistance protein TIR domain reveals interfaces for self-association, signaling, and autoregulation. Cell Host Microbe **9,** 200-211.

Brommonschenkel, S.H., Frary, A., Frary, A., and Tanksley, S.D. (2000). The broad-spectrum tospovirus resistance gene Sw-5 of tomato is a homolog of the root-knot nematode resistance gene Mi. Mol Plant Microbe Interact **13,** 1130-1138.

Burch-Smith, T.M., Schiff, M., Caplan, J.L., Tsao, J., Czymmek, K., and Dinesh-Kumar, S.P. (2007). A novel role for the TIR domain in association with pathogen-derived elicitors. PLoS Biol **5,** e68.

Canto, T., and Palukaitis, P. (2002). Novel N gene-associated, temperature-independent resistance to the movement of tobacco mosaic virus vectors neutralized by a cucumber mosaic virus RNA1 transgene. J Virol **76,** 12908-12916.

Caplan, J., Padmanabhan, M., and Dinesh-Kumar, S.P. (2008a). Plant NB-LRR Immune Receptors: From Recognition to Transcriptional Reprogramming. Cell host & microbe **3,** 126-135.

Caplan, J.L., Mamillapalli, P., Burch-Smith, T.M., Czymmek, K., and Dinesh-Kumar, S.P. (2008b). Chloroplastic protein NRIP1 mediates innate immune receptor recognition of a viral effector. Cell **132,** 449-462.

Cesari, S., Moore, J., Chen, C., Webb, D., Periyannan, S., Mago, R., Bernoux, M., Lagudah, E.S., and Dodds, P.N. (2016). Cytosolic activation of cell death and stem rust resistance by cereal MLA-family CC-NLR proteins. Proc Natl Acad Sci U S A **113,** 10204-10209.

Chen, T., Liu, D., Niu, X., Wang, J., Qian, L., Han, L., Liu, N., Zhao, J., Hong, Y., and Liu, Y. (2017). Antiviral Resistance Protein Tm-2(2) Functions on the Plasma Membrane. Plant Physiol **173,** 2399-2410.

Chen, X., Zhu, M., Jiang, L., Zhao, W., Li, J., Wu, J., Li, C., Bai, B., Lu, G., Chen, H., Moffett, P., and Tao, X. (2016). A multilayered regulatory mechanism for the autoinhibition and activation of a plant CC-NB-LRR resistance protein with an extra N-terminal domain. New Phytol **212,** 161-175.

Cheng, Y.T., Germain, H., Wiermer, M., Bi, D., Xu, F., Garcia, A.V., Wirthmueller, L., Despres, C., Parker, J.E., Zhang, Y., and Li, X. (2009). Nuclear pore complex component MOS7/Nup88 is required for innate immunity and nuclear accumulation of defense regulators in Arabidopsis. Plant Cell **21,** 2503-2516.

Chook, Y.M., and Blobel, G. (2001). Karyopherins and nuclear import. Current opinion in structural biology **11,** 703-715.

Coll, N.S., Vercammen, D., Smidler, A., Clover, C., Van Breusegem, F., Dangl, J.L., and Epple, P. (2010). Arabidopsis type I metacaspases control cell death. Science **330,** 1393-1397.

Collier, S.M., and Moffett, P. (2009). NB-LRRs work a "bait and switch" on pathogens. Trends Plant Sci **14,** 521-529.

Collier, S.M., Hamel, L.P., and Moffett, P. (2011). Cell death mediated by the N-terminal domains of a unique and highly conserved class of NB-LRR protein. Mol Plant Microbe Interact **24,** 918-931.

Cui, H., Tsuda, K., and Parker, J.E. (2015). Effector-triggered immunity: from pathogen perception to robust defense. Annu Rev Plant Biol **66,** 487-511.

De Oliveira, A.S., Koolhaas, I., Boiteux, L.S., Caldararu, O.F., Petrescu, A.J., Oliveira Resende, R., and Kormelink, R. (2016). Cell death triggering and effector recognition by Sw-5 SD-CNL proteins from resistant and susceptible tomato isolines to Tomato spotted wilt virus. Mol Plant Pathol **17,** 1442-1454.

Deom, C.M., Wolf, S., Holt, C.A., Lucas, W.J., and Beachy, R.N. (1991). Altered function of the tobacco mosaic virus movement protein in a hypersensitive host. Virology **180,** 251-256.

Deslandes, L., Olivier, J., Peeters, N., Feng, D.X., Khounlotham, M., Boucher, C., Somssich, I., Genin, S., and Marco, Y. (2003). Physical interaction between RRS1-R, a protein conferring resistance to bacterial wilt, and PopP2, a type III effector targeted to the plant nucleus. Proc Natl Acad Sci U S A **100,** 8024-8029.

Dodds, P.N., and Rathjen, J.P. (2010). Plant immunity: towards an integrated view of plant-pathogen interactions. Nat Rev Genet **11,** 539-548.

Ea, V.D.B., and Jones, J.D. (1998). Plant disease-resistance proteins and the gene-for-gene concept. Trends in Biochemical Sciences **23,** 454-456(453).

Engelhardt, S., Boevink, P.C., Armstrong, M.R., Ramos, M.B., Hein, I., and Birch, P.R. (2012). Relocalization of late blight resistance protein R3a to endosomal compartments is associated with effector recognition and required for the immune response. Plant Cell **24,** 5142-5158.

Ernst, K., Kumar, A., Kriseleit, D., Kloos, D.U., Phillips, M.S., and Ganal, M.W. (2002). The broad-spectrum potato cyst nematode resistance gene (Hero) from tomato is the only member of a large gene family of NBS-LRR genes with an unusual amino acid repeat in the LRR region. Plant J **31,** 127-136.

Feng, M., Cheng, R., Chen, M., Guo, R., Li, L., Feng, Z., Wu, J., Xie, L., Hong, J., Zhang, Z., Kormelink, R., and Tao, X. (2020). Rescue of tomato spotted wilt virus entirely from complementary DNA clones. Proc Natl Acad Sci U S A **117,** 1181-1190.

Feng, Z., Xue, F., Xu, M., Chen, X., Zhao, W., Garcia-Murria, M.J., Mingarro, I., Liu, Y., Huang, Y., Jiang, L., Zhu, M., and Tao, X. (2016). The ER-Membrane Transport System Is Critical for Intercellular Trafficking of the NSm Movement Protein and Tomato Spotted Wilt Tospovirus. PLoS Pathog **12,** e1005443.

Gao, Z., Chung, E.H., Eitas, T.K., and Dangl, J.L. (2011). Plant intracellular innate immune receptor Resistance to Pseudomonas syringae pv. maculicola 1 (RPM1) is activated at, and functions on, the plasma membrane. Proc Natl Acad Sci U S A **108,** 7619-7624.

Garcia, A.V., Blanvillain-Baufume, S., Huibers, R.P., Wiermer, M., Li, G., Gobbato, E., Rietz, S., and Parker, J.E. (2010). Balanced nuclear and cytoplasmic activities of EDS1 are required

for a complete plant innate immune response. PLoS Pathog **6,** e1000970.

Gassmann, W. (2005). Natural variation in the Arabidopsis response to the avirulence gene hopPsyA uncouples the hypersensitive response from disease resistance. Mol Plant Microbe Interact **18,** 1054-1060.

Hallwass, M., de Oliveira, A.S., de Campos Dianese, E., Lohuis, D., Boiteux, L.S., Inoue-Nagata, A.K., Resende, R.O., and Kormelink, R. (2014). The Tomato spotted wilt virus cell-to-cell movement protein (NSM) triggers a hypersensitive response in Sw-5-containing resistant tomato lines and in Nicotiana benthamiana transformed with the functional Sw-5b resistance gene copy. Mol Plant Pathol **15,** 871-880.

Heidrich, K., Wirthmueller, L., Tasset, C., Pouzet, C., Deslandes, L., and Parker, J.E. (2011). Arabidopsis EDS1 connects pathogen effector recognition to cell compartment-specific immune responses. Science **334,** 1401-1404.

Heinlein, M. (2015). Plant virus replication and movement. Virology **479-480,** 657-671.

Horsefield, S., Burdett, H., Zhang, X., Manik, M.K., Shi, Y., Chen, J., Qi, T., Gilley, J., Lai, J.S., Rank, M.X., Casey, L.W., Gu, W., Ericsson, D.J., Foley, G., Hughes, R.O., Bosanac, T., von Itzstein, M., Rathjen, J.P., Nanson, J.D., Boden, M., Dry, I.B., Williams, S.J., Staskawicz, B.J., Coleman, M.P., Ve, T., Dodds, P.N., and Kobe, B. (2019). NAD(+) cleavage activity by animal and plant TIR domains in cell death pathways. Science **365,** 793-799.

Inoue, H., Hayashi, N., Matsushita, A., Xinqiong, L., Nakayama, A., Sugano, S., Jiang, C.J., and Takatsuji, H. (2013). Blast resistance of CC-NB-LRR protein Pb1 is mediated by WRKY45 through protein-protein interaction. Proc Natl Acad Sci U S A **110,** 9577-9582.

Jones, J.D., Vance, R.E., and Dangl, J.L. (2016). Intracellular innate immune surveillance devices in plants and animals. Science **354**.

Jubic, L.M., Saile, S., Furzer, O.J., El Kasmi, F., and Dangl, J.L. (2019). Help wanted: helper NLRs and plant immune responses. Curr Opin Plant Biol **50,** 82-94.

Kanneganti, T.D., Bai, X., Tsai, C.W., Win, J., Meulia, T., Goodin, M., Kamoun, S., and Hogenhout, S.A. (2007). A functional genetic assay for nuclear trafficking in plants. Plant J **50,** 149-158.

Kapos, P., Devendrakumar, K.T., and Li, X. (2019). Plant NLRs: From discovery to application. Plant Sci **279,** 3-18.

Katagiri, F., and Tsuda, K. (2010). Understanding the plant immune system. Mol Plant Microbe Interact **23,** 1531-1536.

Kawano, Y., Fujiwara, T., Yao, A., Housen, Y., Hayashi, K., and Shimamoto, K. (2014). Palmitoylation-dependent membrane localization of the rice resistance protein pit is critical for the activation of the small GTPase OsRac1. J Biol Chem **289,** 19079-19088.

Kong, L., Qiu, X., Kang, J., Wang, Y., Chen, H., Huang, J., Qiu, M., Zhao, Y., Kong, G., Ma, Z., Wang, Y., Ye, W., Dong, S., Ma, W., and Wang, Y. (2017). A Phytophthora Effector Manipulates Host Histone Acetylation and Reprograms Defense Gene Expression to Promote Infection. Curr Biol **27,** 981-991.

Kormelink, R., Storms, M., Van Lent, J., Peters, D., and Goldbach, R. (1994). Expression and subcellular location of the NSM protein of tomato spotted wilt virus (TSWV), a putative viral movement protein. Virology **200,** 56-65.

Kormelink, R., Garcia, M.L., Goodin, M., Sasaya, T., and Haenni, A.L. (2011). Negative-strand

RNA viruses: the plant-infecting counterparts. Virus research **162,** 184-202.

Kourelis, J., and van der Hoorn, R.A.L. (2018). Defended to the Nines: 25 Years of Resistance Gene Cloning Identifies Nine Mechanisms for R Protein Function. Plant Cell **30,** 285-299.

Krasileva, K.V., Dahlbeck, D., and Staskawicz, B.J. (2010). Activation of an Arabidopsis resistance protein is specified by the in planta association of its leucine-rich repeat domain with the cognate oomycete effector. Plant Cell **22,** 2444-2458.

Lanford, R.E., and Butel, J.S. (1984). Construction and characterization of an SV40 mutant defective in nuclear transport of T antigen. Cell **37,** 801-813.

Lapin, D., Bhandari, D.D., and Parker, J.E. (2020). Origins and Immunity Networking Functions of EDS1 Family Proteins. Annu Rev Phytopathol **58,** 253-276.

Leastro, M.O., Pallas, V., Resende, R.O., and Sanchez-Navarro, J.A. (2017). The functional analysis of distinct tospovirus movement proteins (NSM) reveals different capabilities in tubule formation, cell-to-cell and systemic virus movement among the tospovirus species. Virus research **227,** 57-68.

Li, J., Huang, H., Zhu, M., Huang, S., Zhang, W., Dinesh-Kumar, S.P., and Tao, X. (2019). A Plant Immune Receptor Adopts a Two-Step Recognition Mechanism to Enhance Viral Effector Perception. Mol Plant **12,** 248-262.

Li, W., Zhao, Y., Liu, C., Yao, G., Wu, S., Hou, C., Zhang, M., and Wang, D. (2012). Callose deposition at plasmodesmata is a critical factor in restricting the cell-to-cell movement of Soybean mosaic virus. Plant cell reports **31,** 905-916.

Li, X., Kapos, P., and Zhang, Y. (2015). NLRs in plants. Curr Opin Immunol **32,** 114-121.

Lopez, C., Aramburu, J., Galipienso, L., Soler, S., Nuez, F., and Rubio, L. (2011). Evolutionary analysis of tomato Sw-5 resistance-breaking isolates of Tomato spotted wilt virus. J Gen Virol **92,** 210-215.

Lucas, W.J. (2006). Plant viral movement proteins: agents for cell-to-cell trafficking of viral genomes. Virology **344,** 169-184.

Lukasik-Shreepaathy, E., Slootweg, E., Richter, H., Goverse, A., Cornelissen, B.J., and Takken, F.L. (2012). Dual regulatory roles of the extended N terminus for activation of the tomato MI-1.2 resistance protein. Mol Plant Microbe Interact **25,** 1045-1057.

Ma, S., Lapin, D., Liu, L., Sun, Y., Song, W., Zhang, X., Logemann, E., Yu, D., Wang, J., Jirschitzka, J., Han, Z., Schulze-Lefert, P., Parker, J.E., and Chai, J. (2020). Direct pathogen-induced assembly of an NLR immune receptor complex to form a holoenzyme. Science **370**.

Ma, Y., Guo, H., Hu, L., Martinez, P.P., Moschou, P.N., Cevik, V., Ding, P., Duxbury, Z., Sarris, P.F., and Jones, J.D.G. (2018). Distinct modes of derepression of an Arabidopsis immune receptor complex by two different bacterial effectors. Proceedings of the National Academy of Sciences of the United States of America **115,** 10218-10227.

Ma, Z., Song, T., Zhu, L., Ye, W., Wang, Y., Shao, Y., Dong, S., Zhang, Z., Dou, D., Zheng, X., Tyler, B.M., and Wang, Y. (2015). A Phytophthora sojae Glycoside Hydrolase 12 Protein Is a Major Virulence Factor during Soybean Infection and Is Recognized as a PAMP. Plant Cell **27,** 2057-2072.

Ma, Z., Zhu, L., Song, T., Wang, Y., Zhang, Q., Xia, Y., Qiu, M., Lin, Y., Li, H., Kong, L., Fang, Y., Ye, W., Wang, Y., Dong, S., Zheng, X., Tyler, B.M., and Wang, Y. (2017). A paralogous decoy protects Phytophthora sojae apoplastic effector PsXEG1 from a host

inhibitor. Science **355,** 710-714.

Maekawa, T., Cheng, W., Spiridon, L.N., Toller, A., Lukasik, E., Saijo, Y., Liu, P., Shen, Q.H., Micluta, M.A., Somssich, I.E., Takken, F.L.W., Petrescu, A.J., Chai, J., and Schulze-Lefert, P. (2011). Coiled-coil domain-dependent homodimerization of intracellular barley immune receptors defines a minimal functional module for triggering cell death. Cell Host Microbe **9,** 187-199.

Meier, N., Hatch, C., Nagalakshmi, U., and Dinesh-Kumar, S.P. (2019). Perspectives on intracellular perception of plant viruses. Mol Plant Pathol **20,** 1185-1190.

Meyers, B.C., Kozik, A., Griego, A., Kuang, H., and Michelmore, R.W. (2003). Genome-wide analysis of NBS-LRR-encoding genes in Arabidopsis. Plant Cell **15,** 809-834.

Milligan, S.B., Bodeau, J., Yaghoobi, J., Kaloshian, I., Zabel, P., and Williamson, V.M. (1998). The root knot nematode resistance gene Mi from tomato is a member of the leucine zipper, nucleotide binding, leucine-rich repeat family of plant genes. Plant Cell **10,** 1307-1319.

Mittler, R., Herr, E.H., Orvar, B.L., van Camp, W., Willekens, H., Inze, D., and Ellis, B.E. (1999). Transgenic tobacco plants with reduced capability to detoxify reactive oxygen intermediates are hyperresponsive to pathogen infection. Proc Natl Acad Sci U S A **96,** 14165-14170.

Oliver, J.E., and Whitfield, A.E. (2016). The Genus Tospovirus: Emerging Bunyaviruses that Threaten Food Security. Annual review of virology **3,** 101-124.

Padmanabhan, M.S., Ma, S., Burch-Smith, T.M., Czymmek, K., Huijser, P., and Dinesh-Kumar, S.P. (2013). Novel positive regulatory role for the SPL6 transcription factor in the N TIR-NB-LRR receptor-mediated plant innate immunity. PLoS Pathog **9,** e1003235.

Peiro, A., Canizares, M.C., Rubio, L., Lopez, C., Moriones, E., Aramburu, J., and Sanchez-Navarro, J. (2014). The movement protein (NSm) of Tomato spotted wilt virus is the avirulence determinant in the tomato Sw-5 gene-based resistance. Mol Plant Pathol **15,** 802-813.

Qi, D., and Innes, R.W. (2013). Recent Advances in Plant NLR Structure, Function, Localization, and Signaling. Front Immunol **4,** 348.

Qi, D., DeYoung, B.J., and Innes, R.W. (2012). Structure-function analysis of the coiled-coil and leucine-rich repeat domains of the RPS5 disease resistance protein. Plant Physiol **158,** 1819-1832.

Rao, A.L.N.C., Y. G , Khan, J. A , Dijkstra, J. (2002). Molecular biology of plant virus movement. Plant Viruses As Molecular Pathogens.

Scholthof, K.B., Adkins, S., Czosnek, H., Palukaitis, P., Jacquot, E., Hohn, T., Hohn, B., Saunders, K., Candresse, T., Ahlquist, P., Hemenway, C., and Foster, G.D. (2011). Top 10 plant viruses in molecular plant pathology. Mol Plant Pathol **12,** 938-954.

Seo, J.K., Kwon, S.J., Cho, W.K., Choi, H.S., and Kim, K.H. (2014). Type 2C protein phosphatase is a key regulator of antiviral extreme resistance limiting virus spread. Scientific reports **4,** 5905.

Seong, K., Seo, E., Witek, K., Li, M., and Staskawicz, B. (2020). Evolution of NLR resistance genes with noncanonical N-terminal domains in wild tomato species. New Phytol **227,** 1530-1543.

Shen, Q.H., Saijo, Y., Mauch, S., Biskup, C., Bieri, S., Keller, B., Seki, H., Ulker, B., Somssich, I.E., and Schulze-Lefert, P. (2007). Nuclear activity of MLA immune receptors links

879 isolate-specific and basal disease-resistance responses. Science **315,** 1098-1103.
880 **Slootweg, E., Roosien, J., Spiridon, L.N., Petrescu, A.J., Tameling, W., Joosten, M., Pomp, R.,**
881 **van Schaik, C., Dees, R., Borst, J.W., Smant, G., Schots, A., Bakker, J., and Goverse, A.**
882 (2010). Nucleocytoplasmic distribution is required for activation of resistance by the potato
883 NB-LRR receptor Rx1 and is balanced by its functional domains. Plant Cell **22,** 4195-4215.
884 **Soosaar, J.L., Burch-Smith, T.M., and Dinesh-Kumar, S.P.** (2005). Mechanisms of plant resistance
885 to viruses. Nat Rev Microbiol **3,** 789-798.
886 **Spassova M I, P.T.W., Folkertsma R T, et al.** (2001). The tomato gene Sw-5 is a member of the
887 coiled coil, nucleotide binding, leucine-rich repeat class of plant resistance genes and confers
888 resistance to TSWV in tobacco. Molecular Breeding. **7(2),** 151.
889 **Swiderski, M.R., Birker, D., and Jones, J.D.** (2009). The TIR domain of TIR-NB-LRR resistance
890 proteins is a signaling domain involved in cell death induction. Mol Plant Microbe Interact **22,**
891 157-165.
892 **Takemoto, D., Rafiqi, M., Hurley, U., Lawrence, G.J., Bernoux, M., Hardham, A.R., Ellis, J.G.,**
893 **Dodds, P.N., and Jones, D.A.** (2012). N-terminal motifs in some plant disease resistance
894 proteins function in membrane attachment and contribute to disease resistance. Mol Plant
895 Microbe Interact **25,** 379-392.
896 **Takken, F.L.W., and Goverse, A.** (2012). How to build a pathogen detector: structural basis of
897 NB-LRR function. Current Opinion in Plant Biology **15,** 375-384.
898 **Taliansky, M., Torrance, L., and Kalinina, N.O.** (2008). Role of plant virus movement proteins.
899 Methods Mol Biol **451,** 33-54.
900 **Tameling, W.I., Nooijen, C., Ludwig, N., Boter, M., Slootweg, E., Goverse, A., Shirasu, K., and**
901 **Joosten, M.H.** (2010). RanGAP2 mediates nucleocytoplasmic partitioning of the NB-LRR
902 immune receptor Rx in the Solanaceae, thereby dictating Rx function. Plant Cell **22,**
903 4176-4194.
904 **Tasset, C., Bernoux, M., Jauneau, A., Pouzet, C., Briere, C., Kieffer-Jacquinod, S., Rivas, S.,**
905 **Marco, Y., and Deslandes, L.** (2010). Autoacetylation of the Ralstonia solanacearum effector
906 PopP2 targets a lysine residue essential for RRS1-R-mediated immunity in Arabidopsis. PLoS
907 Pathog **6,** e1001202.
908 **Turina, M., Kormelink, R., and Resende, R.O.** (2016). Resistance to Tospoviruses in Vegetable
909 Crops: Epidemiological and Molecular Aspects. Annu Rev Phytopathol **54,** 347-371.
910 **van der Vossen, E.A., Gros, J., Sikkema, A., Muskens, M., Wouters, D., Wolters, P., Pereira, A.,**
911 **and Allefs, S.** (2005). The Rpi-blb2 gene from Solanum bulbocastanum is an Mi-1 gene
912 homolog conferring broad-spectrum late blight resistance in potato. Plant J **44,** 208-222.
913 **van Wersch, S., and Li, X.** (2019). Stronger When Together: Clustering of Plant NLR Disease
914 resistance Genes. Trends Plant Sci **24,** 688-699.
915 **van Wersch, S., Tian, L., Hoy, R., Li, X. .** (2020). Plant NLRs: The whistleblowers of
916 plant immunity. Plant communications**,** doi: https://doi.org/10.1016/j.xplc.2019.100016.
917 **Vos, P., Simons, G., Jesse, T., Wijbrandi, J., Heinen, L., Hogers, R., Frijters, A., Groenendijk, J.,**
918 **Diergaarde, P., Reijans, M., Fierens-Onstenk, J., de Both, M., Peleman, J., Liharska, T.,**
919 **Hontelez, J., and Zabeau, M.** (1998). The tomato Mi-1 gene confers resistance to both
920 root-knot nematodes and potato aphids. Nat Biotechnol **16,** 1365-1369.
921 **Vossen, J.H., van Arkel, G., Bergervoet, M., Jo, K.R., Jacobsen, E., and Visser, R.G.** (2016). The
922 Solanum demissum R8 late blight resistance gene is an Sw-5 homologue that has been

deployed worldwide in late blight resistant varieties. Theor Appl Genet **129,** 1785-1796.

Wan, L., Essuman, K., Anderson, R.G., Sasaki, Y., Monteiro, F., Chung, E.H., Osborne Nishimura, E., DiAntonio, A., Milbrandt, J., Dangl, J.L., and Nishimura, M.T. (2019). TIR domains of plant immune receptors are NAD(+)-cleaving enzymes that promote cell death. Science **365,** 799-803.

Wang, A. (2015). Dissecting the molecular network of virus-plant interactions: the complex roles of host factors. Annu Rev Phytopathol **53,** 45-66.

Wang, J., Hu, M., Wang, J., Qi, J., Han, Z., Wang, G., Qi, Y., Wang, H.W., Zhou, J.M., and Chai, J. (2019a). Reconstitution and structure of a plant NLR resistosome conferring immunity. Science **364**.

Wang, J., Wang, J., Hu, M., Wu, S., Qi, J., Wang, G., Han, Z., Qi, Y., Gao, N., Wang, H.W., Zhou, J.M., and Chai, J. (2019b). Ligand-triggered allosteric ADP release primes a plant NLR complex. Science **364**.

Wang, J., Chen, T., Han, M., Qian, L., Li, J., Wu, M., Han, T., Cao, J., Nagalakshmi, U., Rathjen, J.P., Hong, Y., and Liu, Y. (2020). Plant NLR immune receptor Tm-22 activation requires NB-ARC domain-mediated self-association of CC domain. PLoS Pathog **16,** e1008475.

Wen, W., Meinkoth, J.L., Tsien, R.Y., and Taylor, S.S. (1995). Identification of a signal for rapid export of proteins from the nucleus. Cell **82,** 463-473.

Wirthmueller, L., Zhang, Y., Jones, J.D., and Parker, J.E. (2007). Nuclear accumulation of the Arabidopsis immune receptor RPS4 is necessary for triggering EDS1-dependent defense. Curr Biol **17,** 2023-2029.

Zhao, W., Jiang, L., Feng, Z., Chen, X., Huang, Y., Xue, F., Huang, C., Liu, Y., Li, F., Liu, Y., and Tao, X. (2016). Plasmodesmata targeting and intercellular trafficking of Tomato spotted wilt tospovirus movement protein NSm is independent of its function in HR induction. J Gen Virol **97,** 1990-1997.

Zhu, M., van Grinsven, I.L., Kormelink, R., and Tao, X. (2019). Paving the Way to Tospovirus Infection: Multilined Interplays with Plant Innate Immunity. Annu Rev Phytopathol **57,** 41-62.

Zhu, M., Jiang, L., Bai, B., Zhao, W., Chen, X., Li, J., Liu, Y., Chen, Z., Wang, B., Wang, C., Wu, Q., Shen, Q., Dinesh-Kumar, S.P., and Tao, X. (2017). The Intracellular Immune Receptor Sw-5b Confers Broad-Spectrum Resistance to Tospoviruses through Recognition of a Conserved 21-Amino Acid Viral Effector Epitope. Plant Cell **29,** 2214-2232.

FIGURE LEGENDS

Figure 1. Subcellular localization of Sw-5b in *N. benthamiana* and tomato leaf

961 **cells.** (A) A schematic diagram of Sw-5b. (B) Subcellular localization of free YFP,
962 YFP-Sw-5b and autoactive YFP-Sw-5b^{D857V} mutant in *N. benthamiana* leaf cells at 24
963 hours post agro-infiltration (hpai). (C) Subcellular localization of free YFP,
964 YFP-Sw-5b and autoactive YFP-Sw-5b^{D857V} mutant in tomato leaf cells at 24 hpai. N,
965 nucleus; C, cytoplasm. Bar = 10 μm. The numbers in each image indicate the number
966 of cells showing this subcellular localization pattern and the total number of cells
967 examined per treatment. (D) Western blot analysis of YFP-Sw-5b and
968 YFP-Sw-5b^{D857V} accumulation in the total protein (T), cytoplasmic (C), and nuclear
969 (N) fractionations using antibodies against YFP, actin and histone, respectively.
970 Leaves infiltrated with EV were used as a control. The expressions of actin and
971 histone were used as a cytoplasmic and a nuclear marker, respectively. The Ponceau S
972 stained gel was used to show a cytoplasmic marker.
973
974 **Figure 2. Sw-5b activity on HR cell death induction in the cytoplasm and in the**
975 **nucleus.** (A) Confocal images of *N. benthamiana* leaf cells expressing
976 NES-YFP-Sw-5b, nes-YFP-Sw-5b, NLS-YFP-Sw-5b and nls-YFP-Sw-5b fusion,
977 respectively. All the images were taken at 24–36 hpai. The numbers in each image
978 indicate the number of cells showing this subcellular localization pattern and the total
979 number of cells examined per treatment. N, nucleus; C, cytoplasm. Bar = 10 μm. (B)
980 Induction of HR in *N. benthamiana* leaf areas co-expressing NSm and one of the five
981 Sw-5b fusions. The infiltrated *N. benthamiana* leaf was photographed at 2 dpai (left
982 image) and the same leaf was stained with tryphan blue to show the intence of HR cell

983 death (right image). (C) Western blot analysis of YFP-Sw-5b, NES-YFP-Sw-5b,
984 nes-YFP-Sw-5b, NLS-YFP-Sw-5b, and nls-YFP-Sw-5b in the infiltrated *N.*
985 *benthamiana* leaf tissues. These fusions were enriched using the GFP-Trap beads
986 prior to SDS-PAGE, and the resulting blot was probed using an YFP specific antibody.
987 The Ponceau S stained gel was used to show sample loadings. (D) Time course study
988 of ion leakage in the *N. benthamiana* leaf tissues co-expressing NSm and one of the
989 five Sw-5b fusions. The leaf tissues co-expressing NSm and EV were used as controls.
990 Measurements were performed at 4 h intervals starting from 24 hpai to 48 hpai. Error
991 bars were calculated using the data from three biological replicates per treatment per
992 time point.
993
994 **Figure 3. Effects of cytoplasmic and nuclear Sw-5b on inhibition of viral**
995 **replication in *N. benthamiana*.** (A) Schematic representations of TSWV-based
996 mini-genome replicons. $SR_{(+)eGFP}$, a mini-genome replicon expressing TSWV N and
997 eGFP; $L_{(+)opt}$, TSWV L genomic replicon expressing a codon usage optimized TSWV
998 RdRp; NSm, Wild type TSWV NSm expressed by 35S promoter in p2300S vector;
999 $NSm^{H93A\&H94A}$, a movement defective NSm; (-), the negative (genomic)-strand of
1000 tospovirus RNA; 35S, a double 35S promoter; HH, a hammerhead ribozyme; RZ, a
1001 hepatitis delta virus ribozyme; NOS, a nopaline synthase terminator; 35S Ter, a 35S
1002 transcription terminator. (B) Images of *N. benthamiana* leaf tissues co-expressing of
1003 $SR_{(+)eGFP}$, $L_{(+)opt}$, $NSm^{H93A\&H94A}$, and EV, Sw-5b, NES-Sw-5b, nes-Sw-5b,
1004 NLS-Sw-5b, or nls-Sw-5b. All the tissues were imaged at 4 dpai under a fluorescence

1005 microscope. Bar = 400 μm. (C) Western blot analysis of various fusion proteins in leaf
1006 samples shown in panel (B) using an antibody against YFP. The Ponceau S stained
1007 rubisco large subunit was used to show sample loadings.
1008
1009 **Figure 4. Nucleocytoplasm-, cytoplasm- and nuclear-accumulated Sw-5b activity**
1010 **on NSm cell-to-cell movement in *N. benthamiana* leaves.** (A) A schematic diagram
1011 showing a vector expressing both mCherry-HDEL and NSm-GFP. (B) Cell-to-cell
1012 movement of NSm-GFP in the *N. benthamiana* leaves co-expressing mCherry-HDEL,
1013 NSm-GFP and EV, Sw-5b, NES-Sw-5b or NLS-Sw-5b through agro-infiltration. The
1014 *Agrobacterium* culture carrying pmCherry-HDEL//NSm-GFP was first adjusted to
1015 OD_{600} = 0.2, and then diluted 500 times prior to infiltration. Other *Agrobacterium*
1016 cultures were adjusted to OD_{600} = 0.2 prior to use. The numbers in each image
1017 indicate the number of cells showing this cell-to-cell movement pattern and the total
1018 number of cells examined per treatment. Bar = 50 μm.
1019
1020 **Figure 5. Cytoplasmic and nuclear Sw-5b activity on inducing host immunity to**
1021 **TSWV systemic infection.** (A) Systemic infection analysis of TSWV in
1022 NES-YFP-Sw-5b, nes-YFP-Sw-5b, NLS-YFP-Sw-5b, nls-YFP-Sw-5b, YFP-Sw-5b or
1023 EV transgenic *N. benthamiana* plants. Transgenic *N. benthamiana* plants driven by
1024 the 35S promoter were used in this experiment. The inoculated plants were
1025 photographed at 15 dpi. White arrow indicates the systemic leaves showing HR
1026 trailing. White arrow indicate systemic leaves showing mosaic symptoms. (B)

Western blot analyses of NES-YFP-Sw-5b, nes-YFP-Sw-5b, NLS-YFP-Sw-5b, nls-YFP-Sw-5b, and YFP-Sw-5b accumulations in the transgenic *N. benthamiana* lines driven by the 35S promoter . The EV transgenic line was used as a negative control. (C) RT-PCR detection of TSWV infection in the systemic leaves of different transgenic *N. benthamiana* lines at 15 dpi.

Figure 6. Validation of Sw-5b nucleus localization and its role in host immunity to TSWV systemic infection. (A) Expressions of *importin α1* (IMP α1 KD), *α2* (IMP α2 KD), *α1* and *α2* (IMP *α1* & α2 KD), *β* (IMP β KD), *importin α1*, *α2* and *β* (IMP α1 & α2 & βKD) were silenced, respectively, in the YFP-Sw-5b transgenic *N. benthamiana* through VIGS followed by Confocal Microscopy analysis at 26 hpai. N, nucleus; C, cytoplasm. Bar = 10 μm. The numbers in each image indicate the number of cells showing this subcellular localization pattern and the total number of cells examined per treatment. (B) The gene silenced Sw-5b transgenic *N. benthamiana* plants were inoculated with TSWV. The inoculated plants were photographed at 15 dpi. The white arrow indicates HR trailing in systemic leaves. The numbers in each image indicate the number of plants showing this virus-infected phenotype pattern and the total number of plants tested per treatment.

Figure 7. Additive effect of cytoplasmic and nuclear Sw-5b on host immunity to TSWV infection. (A) Schematic representations of constructs: $M_{(-)opt}$-$SR_{(+)eGFP}$ carry both full length TSWV M segment and $SR_{(+)eGFP}$ mini-replicon to express NSm,

TSWV N, and eGFP in the same cell and $L_{(+)opt}$ carrying a full length antigenomic L segment to express a codon usage optimized RdRp ($RdRp_{opt}$). 2x35S, doubled 35S promoter; HH, hammerhead ribozyme; RZ, hepatitis delta virus ribozyme; NOS, nopaline synthase terminator. (B) *N. benthamiana* leaves co-expressing $M_{(-)opt}$-$SR_{(+)eGFP}$, $L_{(+)opt}$ and EV, Sw-5b, NES-Sw-5b, NLS-Sw-5b, or NES-Sw-5b + NLS-Sw-5b at 4 dpai were examined and imaged under a confocal microscope. The numbers in each image indicate the number of leaf areas showed similar expressing patterns and the total number of cells examined per treatment. Bar = 400 μm. (C) Western blot analysis of eGFP accumulation in assayed leaves shown in panel (B) using an GFP specific antibody. The Ponceau S stained Rubisco large subunit gel is used to show sample loadings. (D) Quantification of eGFP accumulation in leaves shown in panel (C).

Figure 8. Subcellular localization patterns of Sw-5b domains. (A) Schematic diagrams showing a full length Sw-5b or its domains fused with an YFP. (B) Confocal images of *N. benthamiana* leaf epidermal cells expressing various YFP fusions. Images were taken at 24 hpai. The numbers in each image indicate the number of cells showing this subcellular localization pattern and the total number of cells examined per treatment. N, nucleus; C, cytoplasm. Bar = 10 μm.

Figure 9. A working model for Sw-5b-induced host immunity against tospovirus infection. Sw-5b induces different defense responses from different cellular

compartments to combat different tospovirus infection steps. Upon recognition of viral NSm in cytoplasm, Sw-5b switches from the autoinhibited state to an activated state. The cytoplasmic Sw-5b induces a strong cell death response and a host defense to inhibit TSWV replication. Some activated Sw-5b are translocated into nucleus by importins. The nuclear-accumulated Sw-5b induces a host defense that weakly inhibits TSWV replication, but strongly blocks virus cell-to-cell and long-distance movement. Combination of cytoplasmic and nuclear Sw-5b induces a synergistic and strong host immunity against tospovirus infection.

Supporting Information Legends

Figure supplemental 1. Sw-5b recognizes TSWV NSm in cytoplasm. (A) Transient expressions of NSm-YFP-NES, NSm-YFP-nes, NSm-YFP-NLS, and NSm-YFP-nls, respectively, in *N. benthamiana* leaves through agro-infiltration. Epidermal cells expressing various fusion proteins were imaged under a confocal microscope at 24 hpai. The numbers in each image indicate the number of cells showing this subcellular localization pattern and the total number of cells examined per treatment. N, nucleus; C, cytoplasm. Bar = 10 μm. (B) Various fusion proteins described in (A) were, individually, co-expressed with Sw-5b in *N. benthamiana* leaves. A representative leaf was photographed at 5 dpai. (C) Western blot analysis of various NSm fusion protein expressions in the assayed *N. benthamiana* leaves using an YFP specific antibody. Leaf areas co-expressing Sw-5b and EV were used as negative controls. The Ponceau S stained Rubisco large subunit gel was used to show sample loadings.

Figure supplemental 2. Analysis of virus replication monitoring system using a TSWV-based mini-genome replicon and a movement defective NSm mutant. (A) $SR_{(+)eGFP}$, $L_{(+)opt}$, VSRs and NSm or $NSm^{H93A\&H94A}$ mutant were transiently co-expressed in *N. benthamiana* leaves through agro-infiltration. The infiltrated leaves were examined and imaged under a confocal microscope at 4 dpai. The numbers in each image indicate the number of cells showing similar expression pattern and the total number of cells examined per treatment. Bar = 400 μm. (B) Western blot analysis of eGFP accumulation in assayed leaves using an YFP specific antibody. Leaves co-expressing $SR_{(+)eGFP}$, $L_{(+)opt}$, VSRs and EV were used as negative controls. The Ponceau S stained Rubisco large subunit gel was used to show sample loadings.

Figure supplemental 3. Effects of nes-Sw-5b and nls-Sw-5b on NSm-GFP cell-to-cell movement. nes-Sw-5b and nls-Sw-5b were, respectively, co-expressed with mCherry-HDEL//NSm-GFP in *N. benthamiana* leaves through agro-infiltration. The Agrobacterium culture carrying pmCherry-HDEL//NSm-GFP was first adjusted to OD_{600} = 0.2 and then further diluted 500 times prior to use. All other Agrobacterium cultures were adjusted to OD_{600} = 0.2 prior to use. The numbers in each image indicate the number of cells showing similar expression pattern and the total number of cells examined per treatment. Bar = 50 μm.

Figure supplemental 4. Effects of cytoplasmic and nuclear Sw-5b on host immunity to TSWV systemic infection. (A) Transgenic *N. benthamiana* lines expressing NES-YFP-Sw-5b, nes-YFP-Sw-5b, NLS-YFP-Sw-5b, nls-YFP-Sw-5b or YFP-Sw-5b, driven by the Sw-5b promoter, were used in this study. The EV transgenic plants were used as controls. The transgenic plants were inoculated with TSWV and photographed at 15 dpi. White arrow indicate the systemic leaves showing HR trailing. White arrowhead indicates the systemic leaves showing mosaic symptoms. (B) RT-PCR detection of TSWV infection in the systemic leaves of the assayed *N. benthamiana* plants at 15 dpi.

Figure supplemental 5. RT-PCR analyses of *importin α1*, *α2* and *β* expressions in the assayed plants and their effects on TSWV systemic infection. (A) Expressions of *importin α1*, *α2*, and *β* in Sw-5b transgenic *N. benthamiana* plants were silenced individually or together using a TRV-based VIGS vector. The gene silencing results were determined through semi-quantitative RT-PCR using gene specific primers. PCR products obtained after 25 cycles of PCR reaction were visualized in 1% agrose gel through electrophoresis. (B) RT-PCR detection of TSWV systemic infection in the assayed plants. The resulting PCR products were visualized in 1% agrose gel through electrophoresis.

Figure supplemental 6. Cytoplasmic and nuclear Sw-5b activity on TSWV-GFP cell-to-cell movement in *N. benthamiana* leaves. (A) $pL_{(+)opt}$ and $pSR_{(+)eGFP}$-$M_{(-)opt}$

1137 were co-inoculated with TSWV-GFP into *Nicotiana benthamiana* leaves through
1138 agro-infiltration. The inoculated leaves were examined and imaged under a confocal
1139 microscope at 4 dpai. Bar = 400 μm. (B) Statistic analysis of TSWV-GFP cell-to-cell
1140 movement in the assayed *N. benthamiana* leaves from Figure 7B. A total of 9 assayed
1141 leaves were used for each treatment.

1142

1143 **Figure supplemental 7. Western blot detection of various YFP-tagged Sw-5b**
1144 **domains in assayed *N. benthamiana* leaves.** The fusion proteins were transiently
1145 expressed, individually, in *N. benthamiana* leaves. The expressed fusion proteins were
1146 detected using an YFP specific antibody. Arrows indicate the positions of the
1147 expressed fusion proteins. The Ponceau S stained Rubisco large subunit gel was used
1148 to show estimate sample loadings.

1149

1150 **Table supplemental 1. Response of six different types of transgenic *Nicotiana***
1151 ***benthamina* plants driven by 35S promoter to TSWV infection**

1152

1153 **Table supplemental 2. Response of six different types of transgenic *Nicotiana***
1154 ***benthamina* plants driven by Sw-5b native promoter to TSWV infection**

1155

1156 **Table supplemental 3. List of primers used in this study**

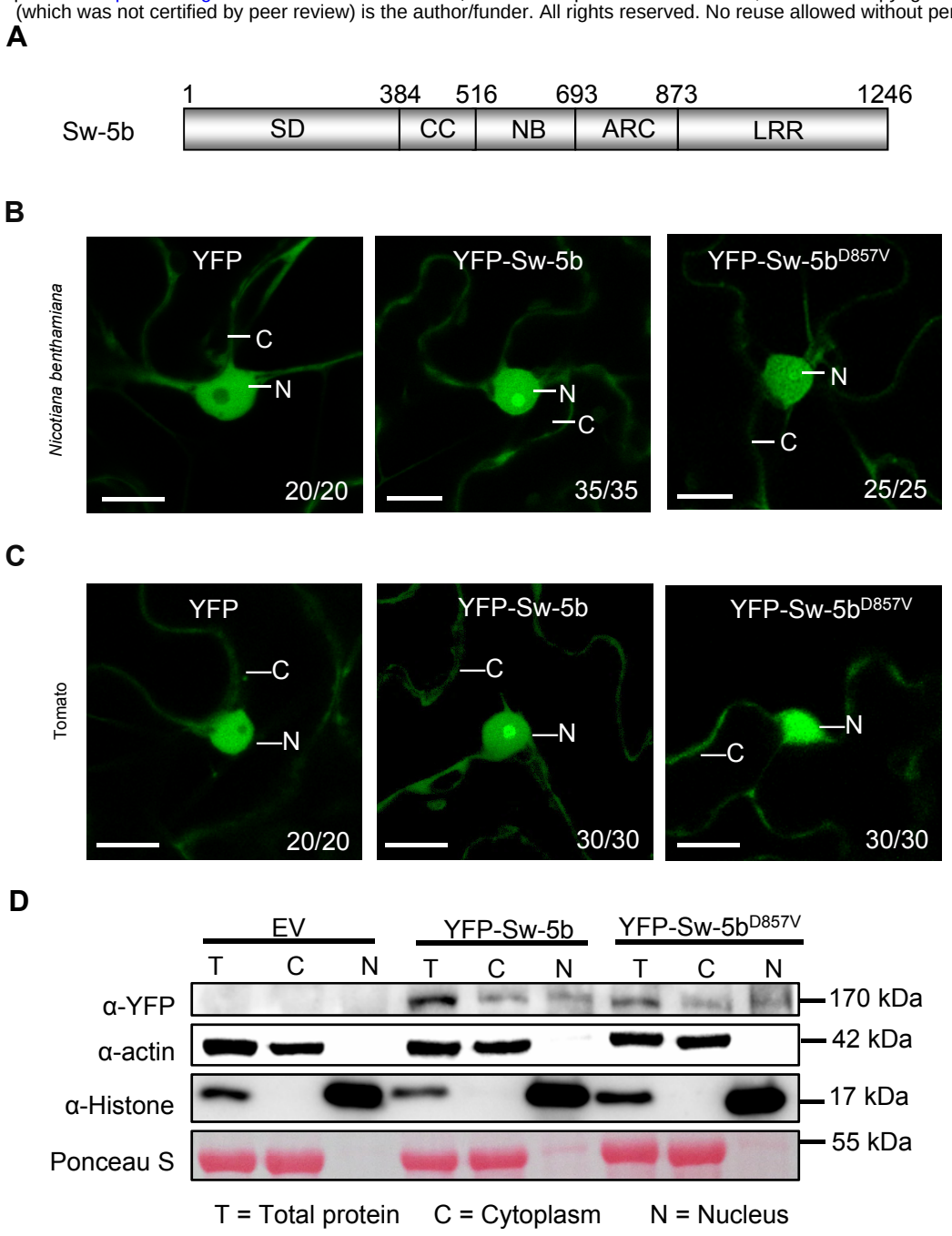

Figure 1.

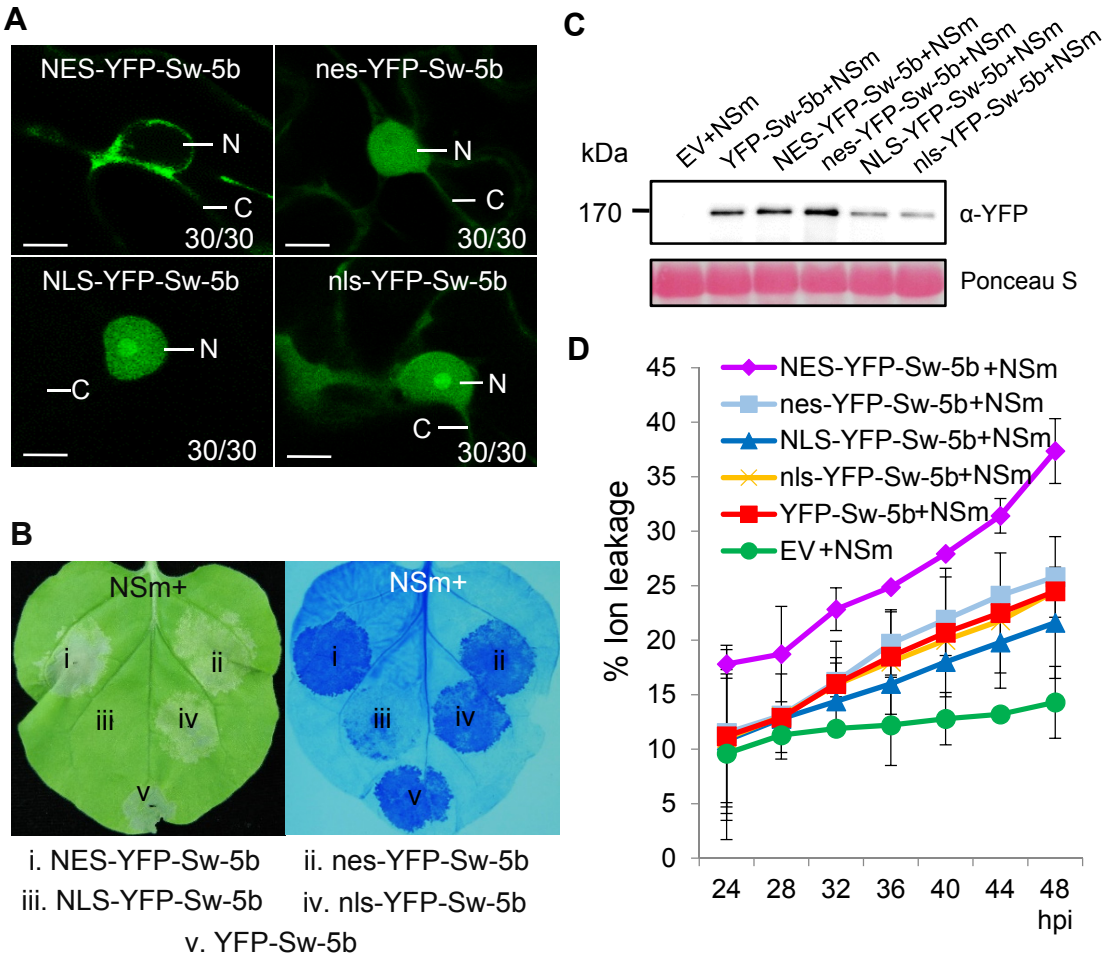

Figure 2.

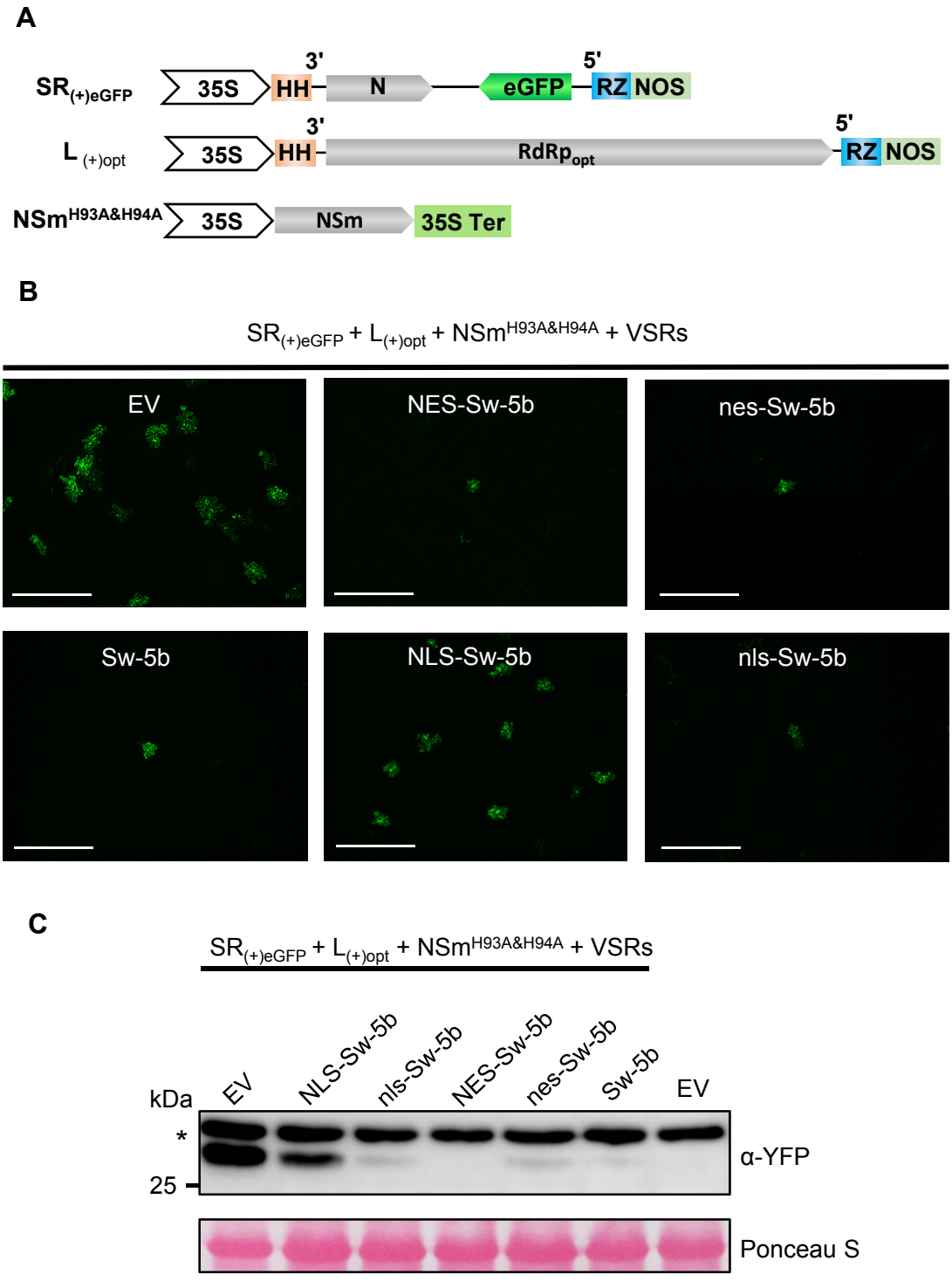

Figure 3.

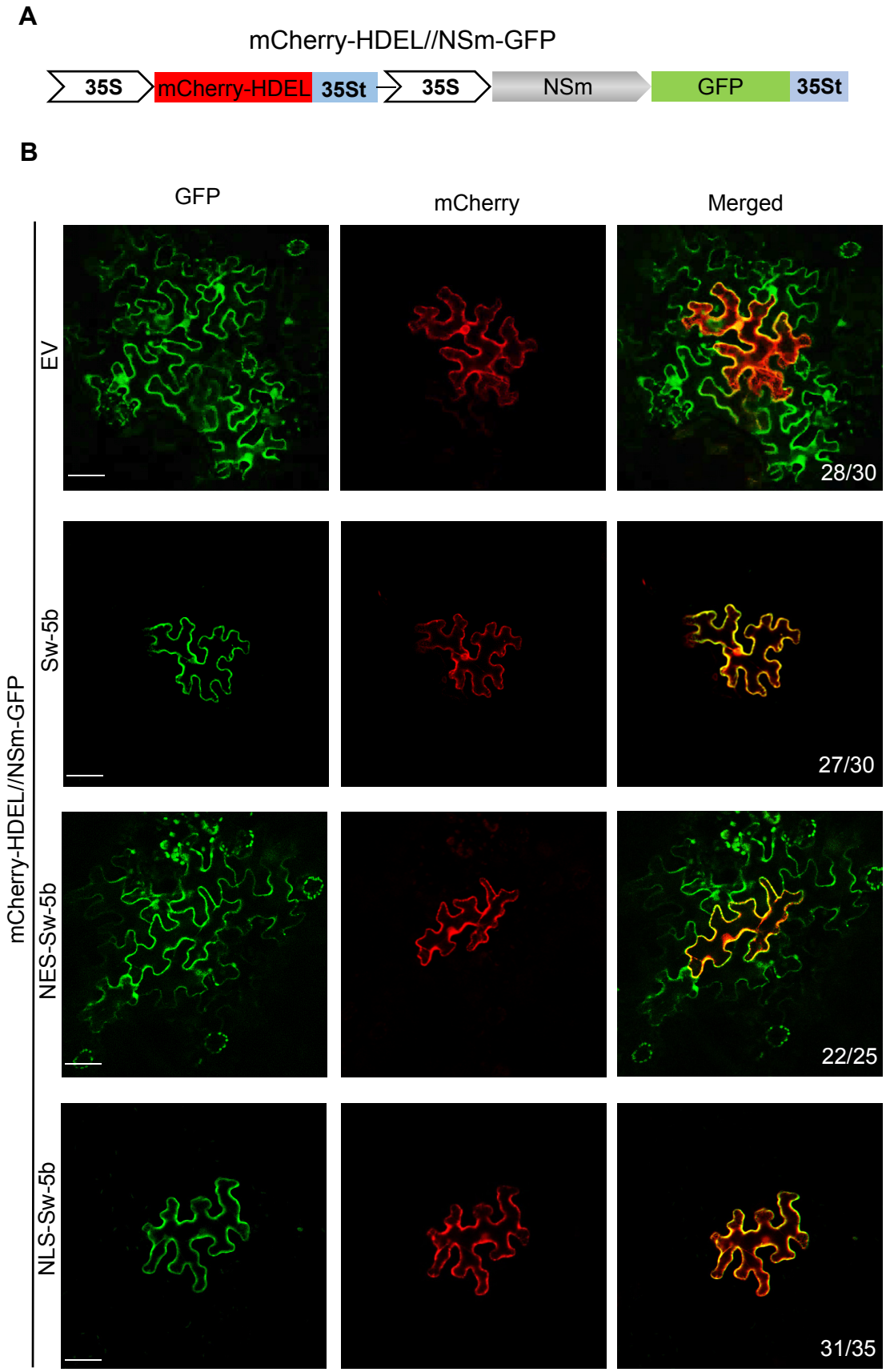

Figure 4.

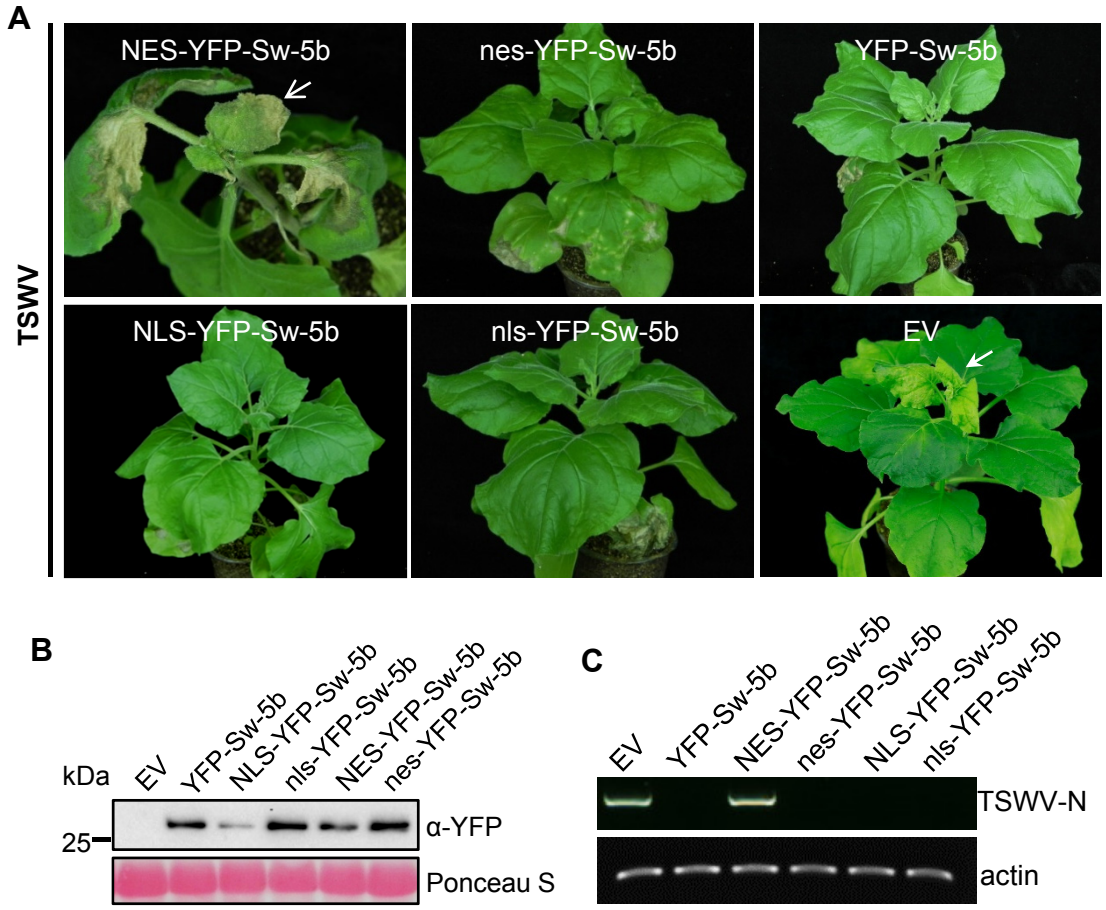

Figure 5.

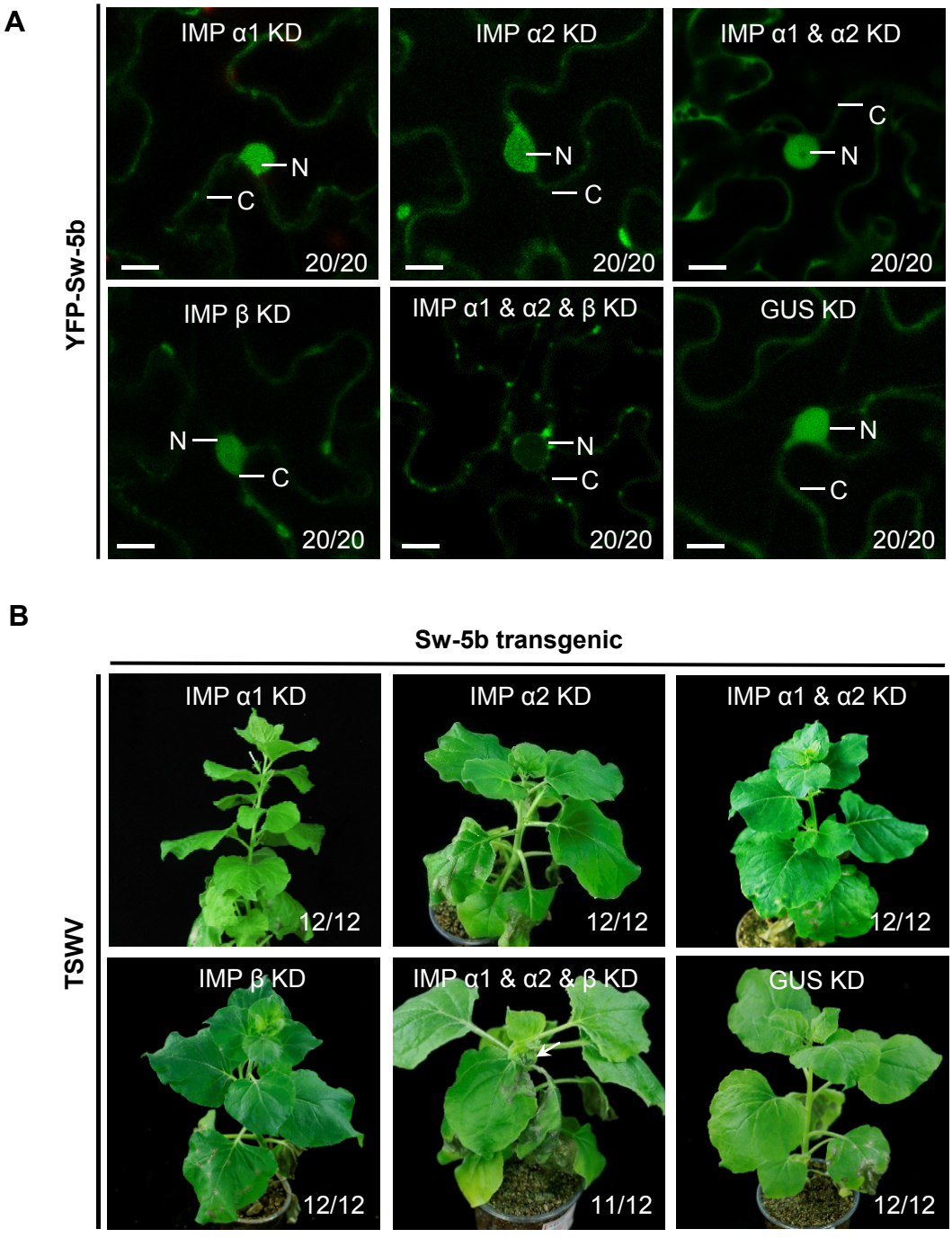

Figure 6

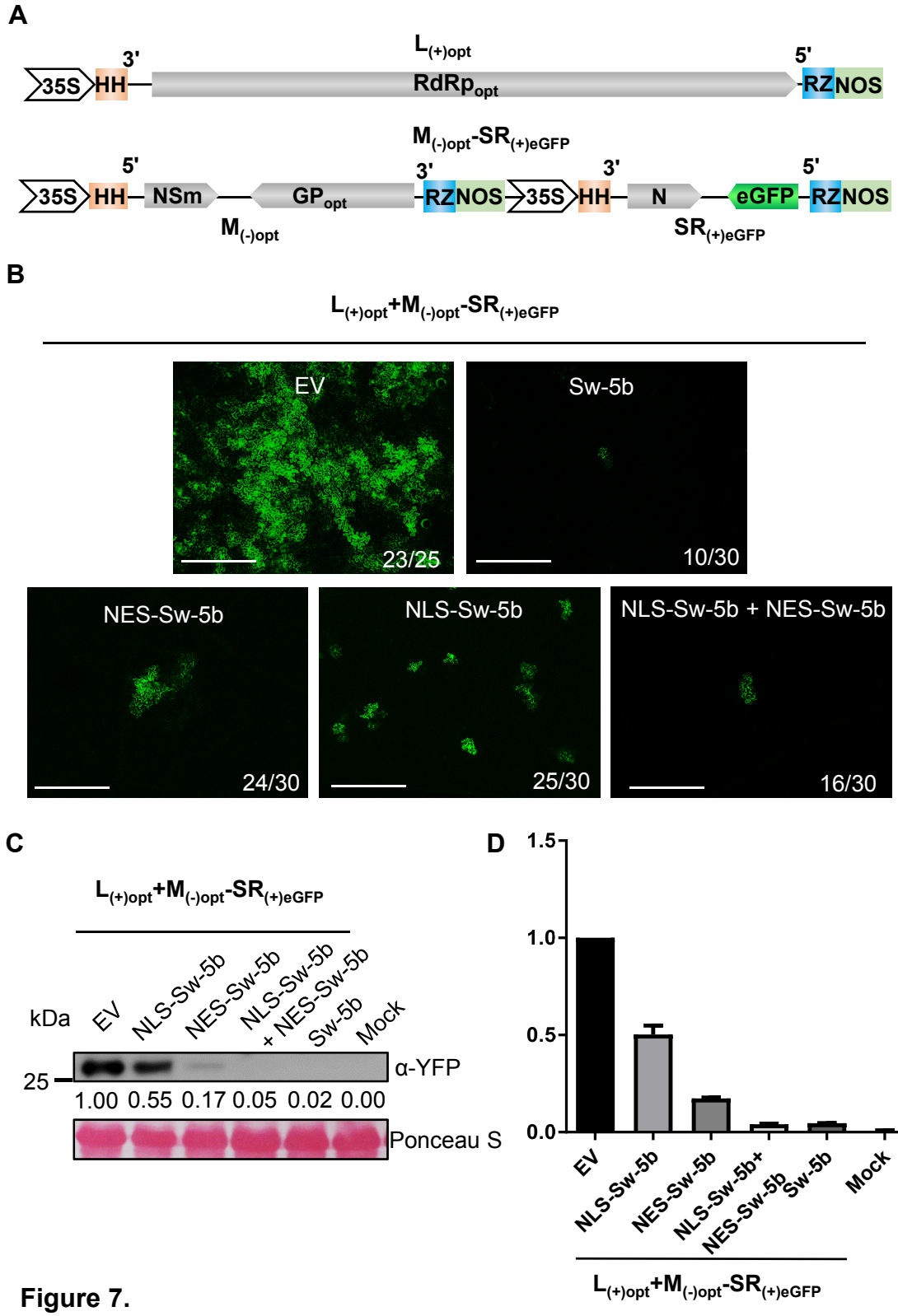

Figure 7.

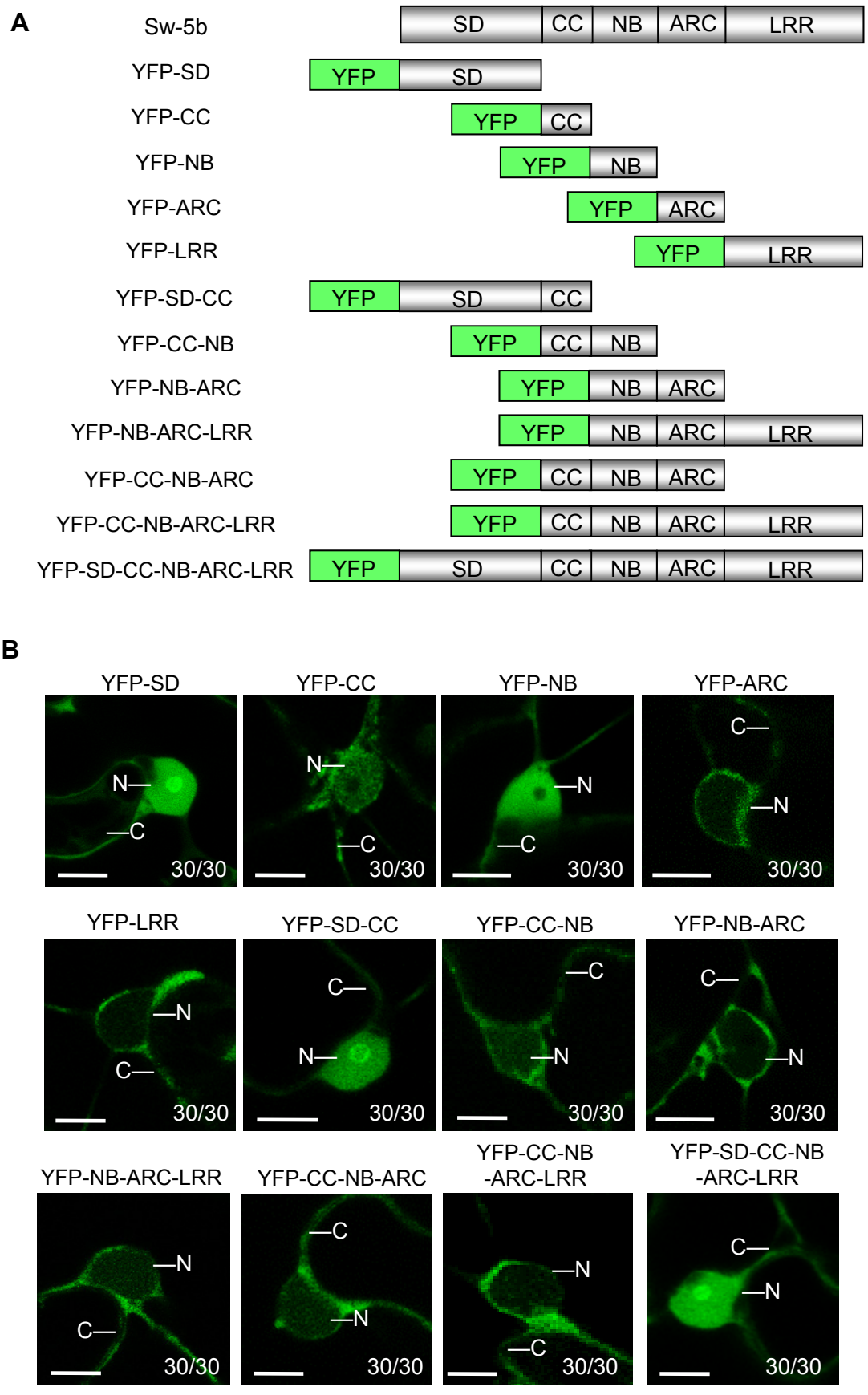

Figure 8.

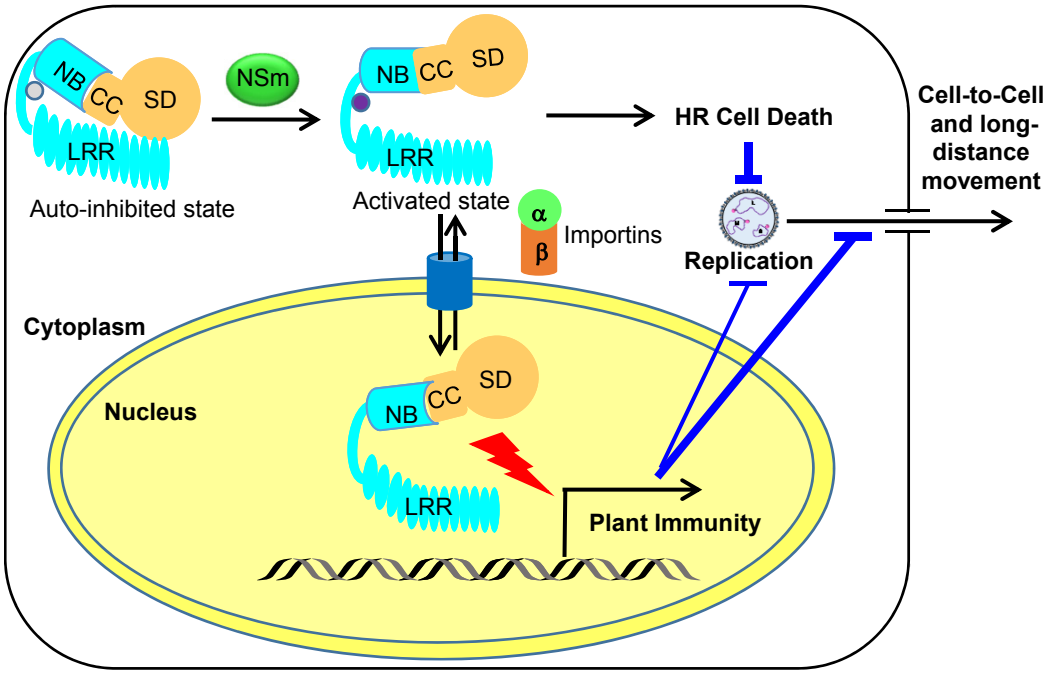

Figure 9.

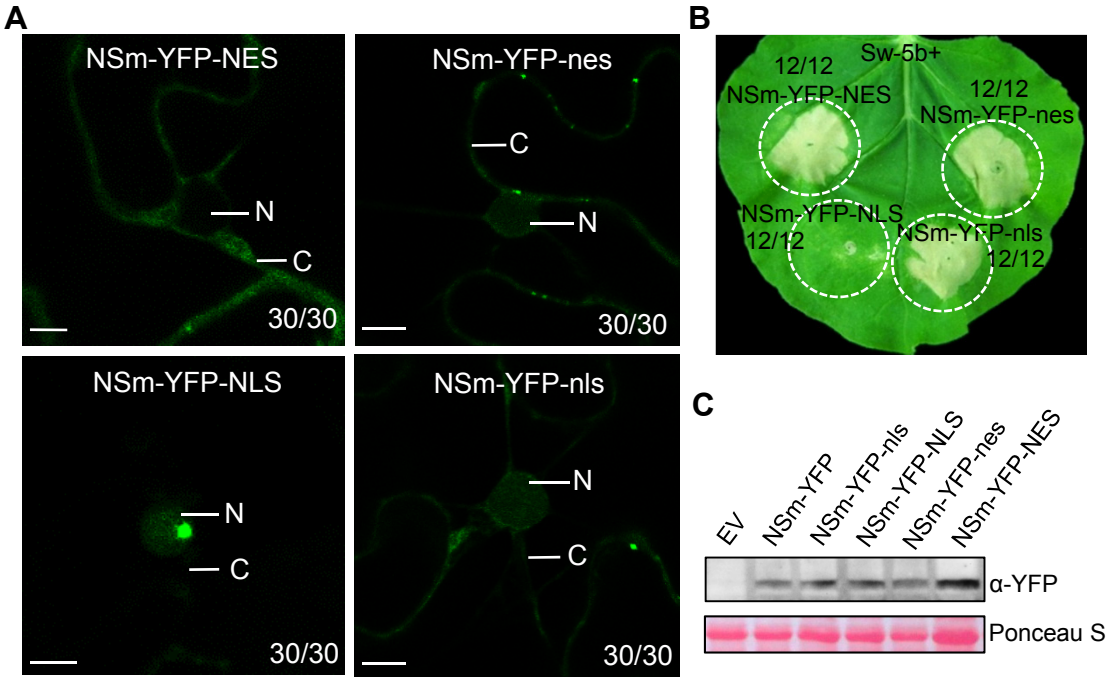

Figure supplement 1.

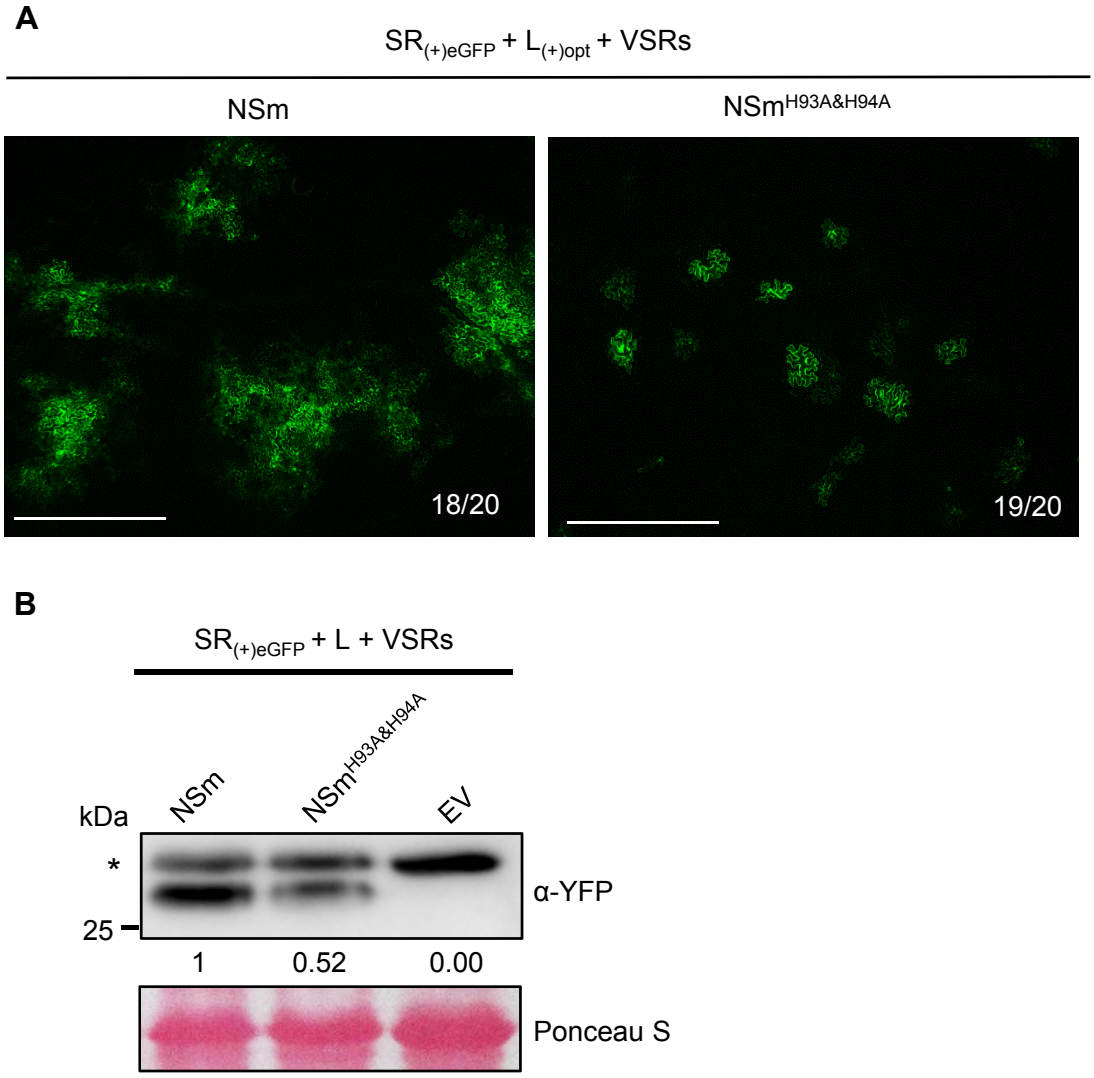

Figure supplement 2.

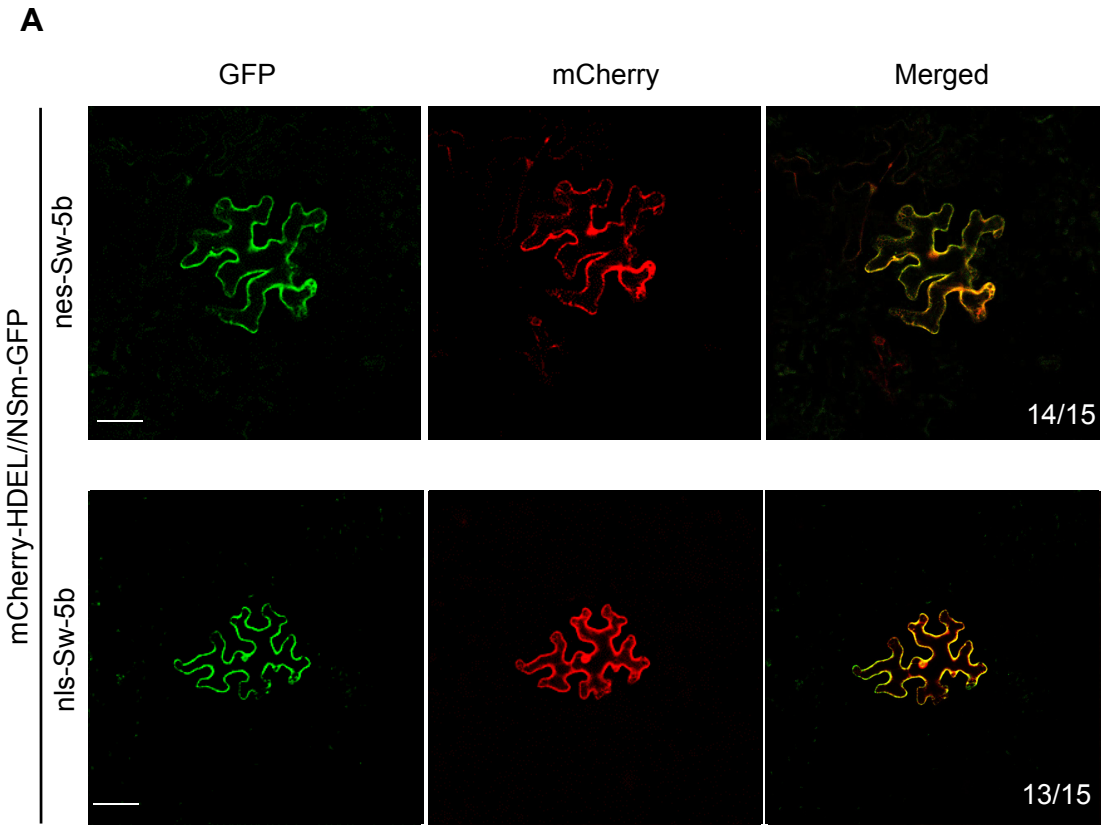

Figure supplement 3.

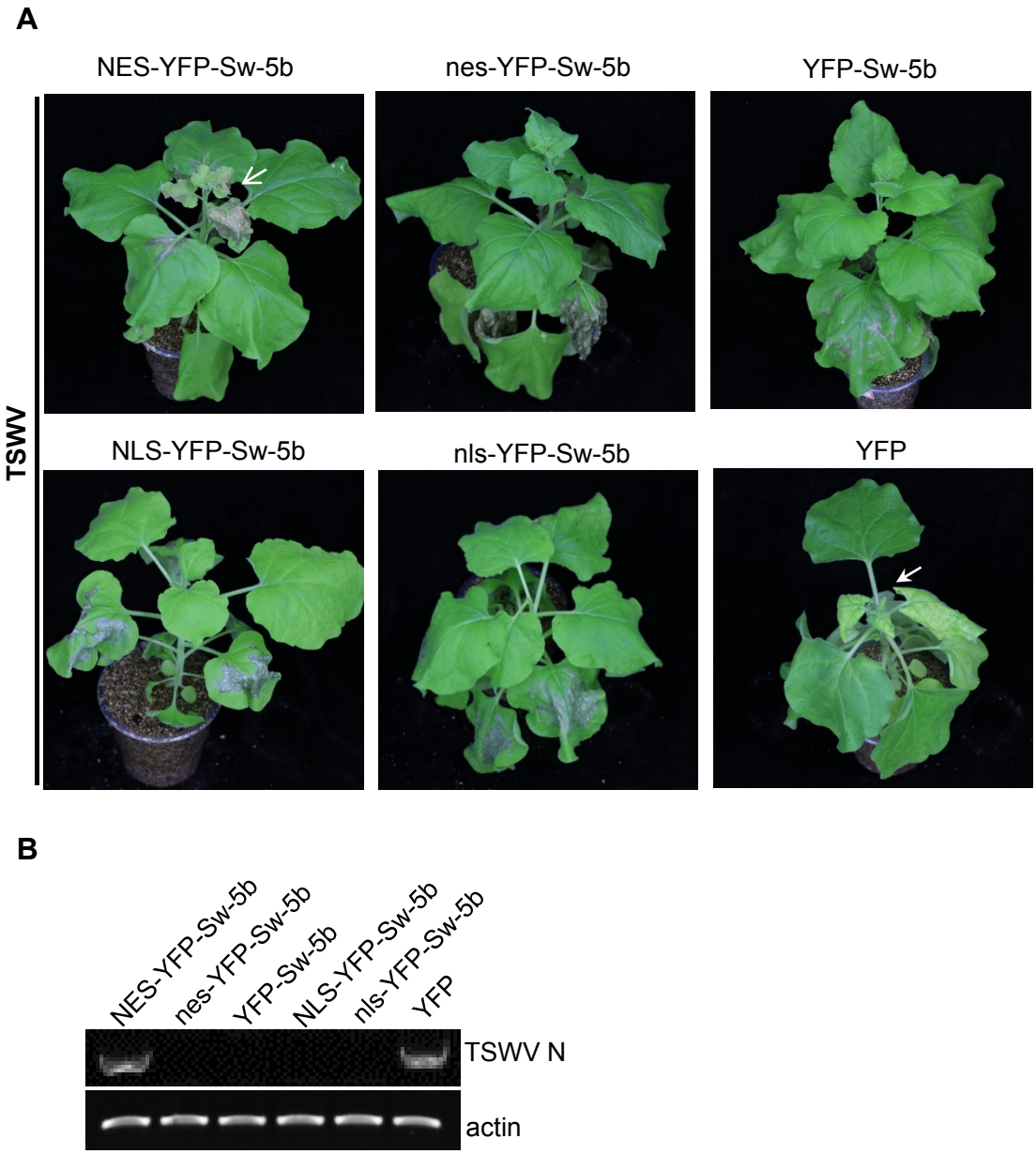

Figure supplement 4.

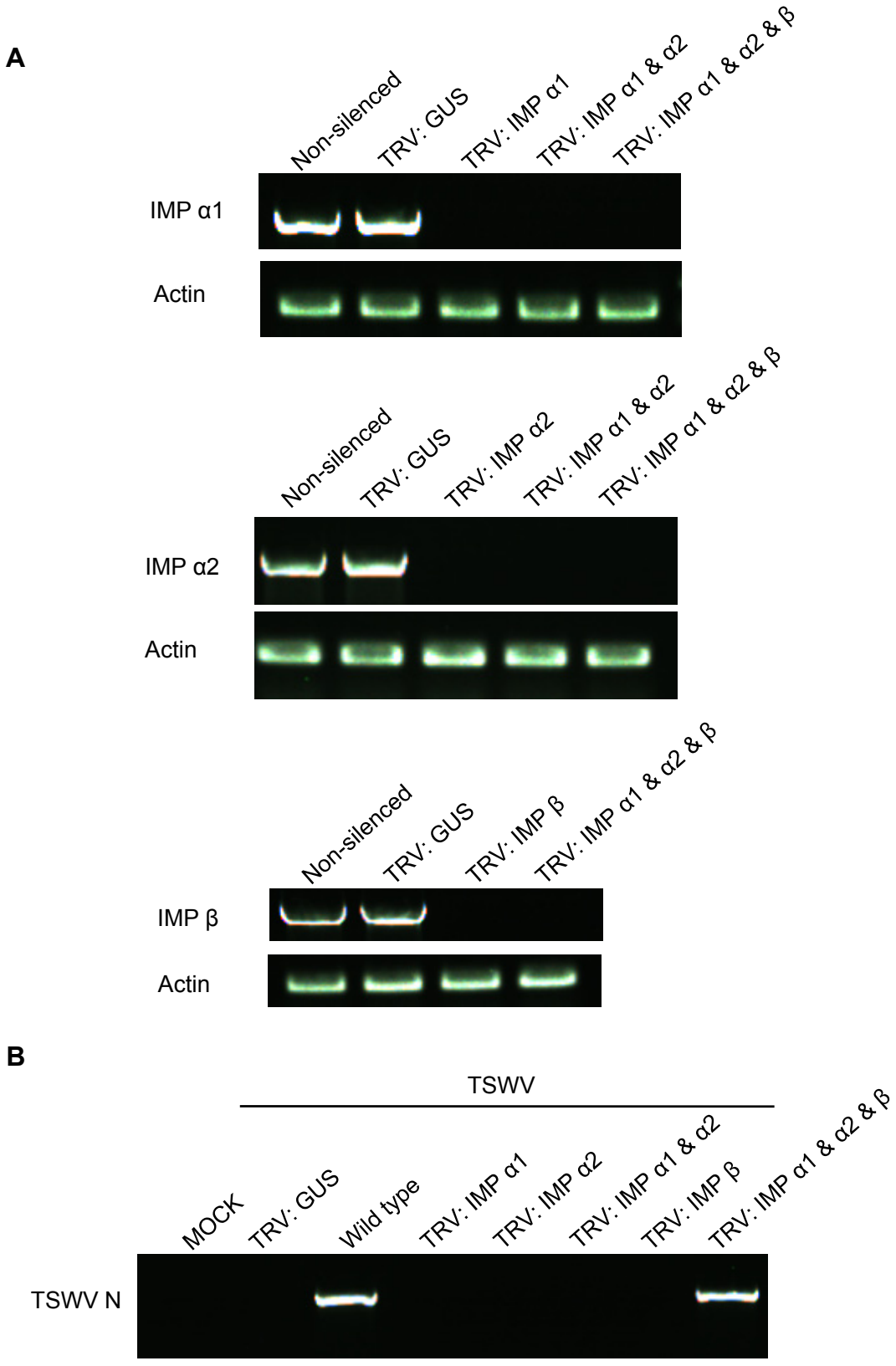

Figure supplement 5.

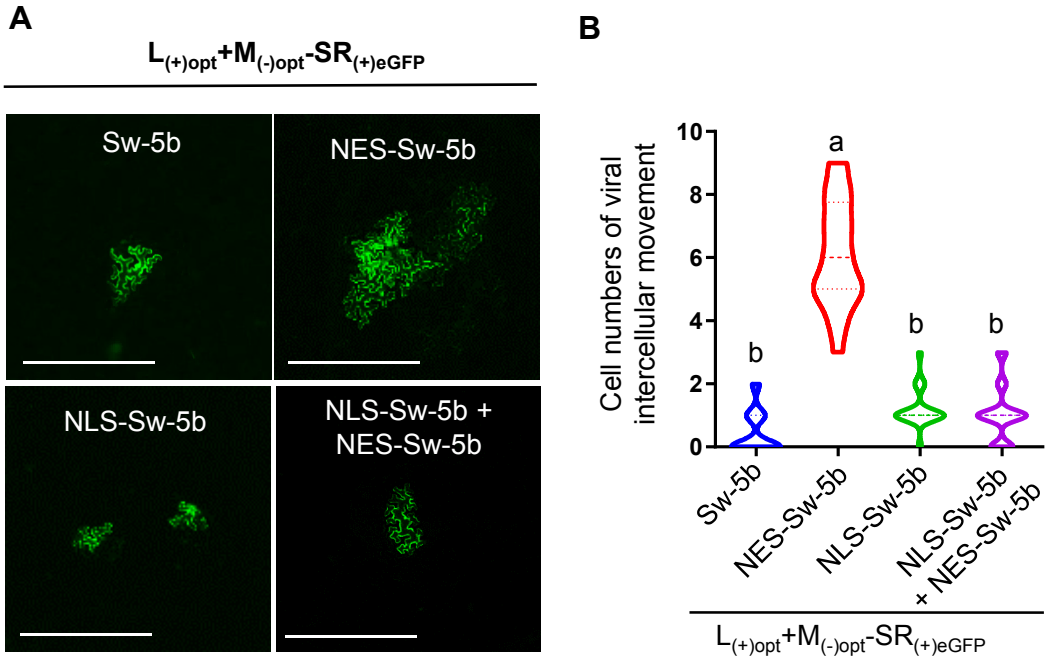

Figure supplement 6.

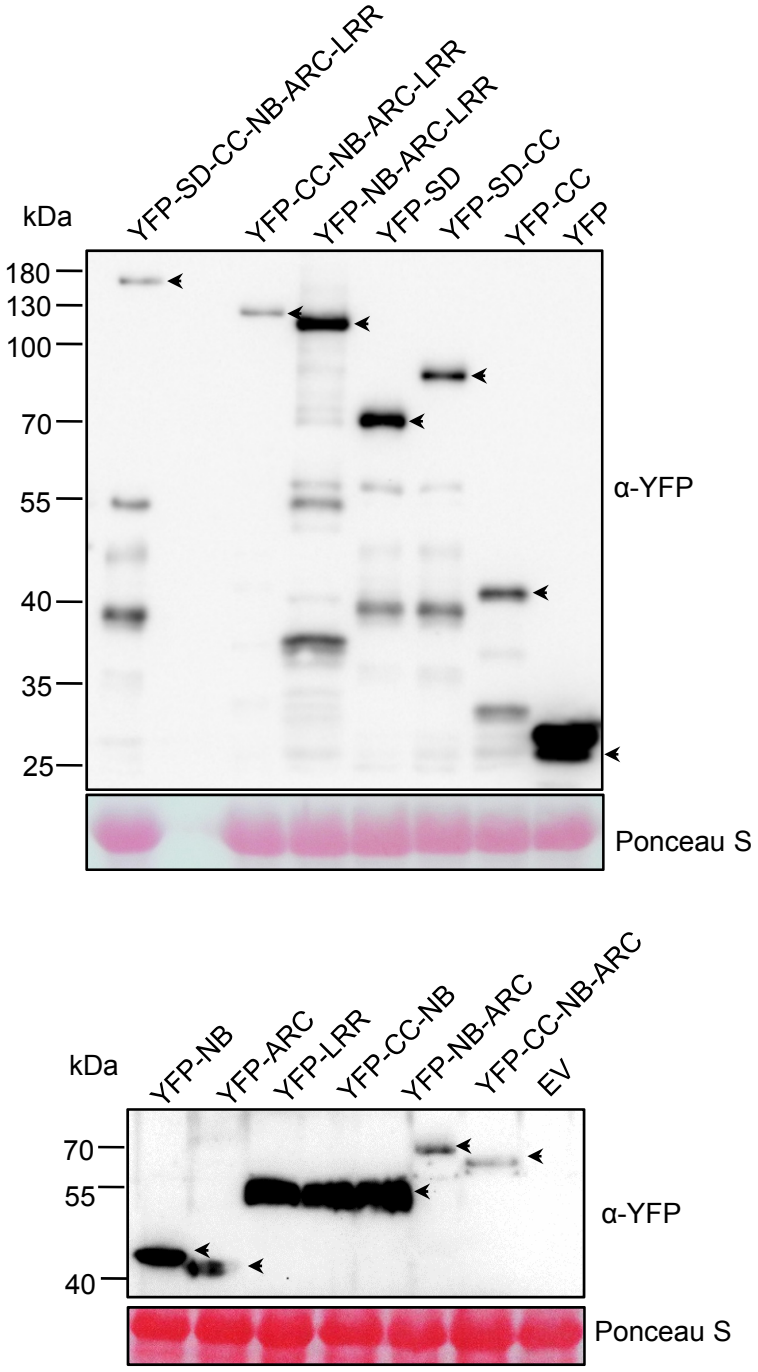

Figure supplement 7.